IN VIVO ASSESSMENT OF BONE HEALING FOLLOWING PIEZOTOME® ULTRASONIC INSTRUMENTATION

Jonathan M. Reside, DDS

A thesis submitted to the faculty of the University of North Carolina at Chapel Hill in partial fulfillment of the requirements for the degree of Master of Science in the Department of Periodontology, School of Dentistry.

Chapel Hill
2012

Approved by:

Dr. Salvador Nares

Dr. Eric Everett

Dr. Ricardo Padilla

Abstract

JONATHAN M. RESIDE: *In vivo* Assessment of Bone Healing Following Piezotome® Ultrasonic Instrumentation
(Under the direction of Salvador Nares, D.D.S., Ph.D., Eric Everett, M.S. Ph.D., Ricardo Padilla, D.D.S.)

The first part of this thesis details a randomized controlled study in which osteotomies were prepared in the tibia of 15 rats using either 1st or 2nd Generation Piezotome® ultrasonic surgical units, or high speed rotary instrumentation. Sham surgeries were performed as controls. Real-time reverse transcriptase polymerase chain reaction was completed, highlighting differential gene expression patterns at 1 week post-surgery while immunohistochemistry staining for matrix metalloproteinase 2, matrix metalloproteinase 8, and tumor necrosis factor-α compared the localization of gene expression at 1 and 3 weeks post-surgery. The second part details a second randomized control study in which osteotomies were prepared in the tibia of 9 rats using the same instrumentation methods. Three weeks post-surgery, micro-computer tomography was completed to evaluate bone mineral density and percentage of bone fill within the osteotomy defects and peripheral bone. Qualitative histological characterization of the tissues was also completed at 3 weeks.

Many thanks to the following people:

Dr. Salvador Nares for his knowledge, leadership, and patience throughout the completion of both this research project and my residency training program.

Dr. Ricardo Padilla for his encouragement, calm demeanor, and level-headedness.

Dr. Eric Everett for his clear direction and incomparable insight.

Dr. Roger Arce for his selfless support.

Dr. Nadine Brodala for steering the direction of my pursuits (both my research endeavors and larger career decisions), for her mentorship, and her friendship.

Dr. Ingeborg De Kok and Dr. Patricia Miguez for their assistance with the surgical procedures.

My parents, Dr. Glenn and Karin Reside, and my brother, Connor, for their limitless support and sacrifice in helping me to achieve my goals.

Robert Schooley for his encouragement, extreme patience, and confidence in me.

Drs. Akshay Kumarswamy and Romina Perri for their friendship and inspiration throughout this residency training program.

Sarah Lowman, Dinushika Mohottige, and Megumi Yamauchi for their humor, encouragement, and friendship.

My fellow residents.

My friends for all of their well-wishes, support, and patience over the years.

TABLE OF CONTENTS

LIST OF TABLES

PART I

PART II

LIST OF FIGURES

PART I

PART II

APPENDIX A

LIST OF ABBREVIATIONS

BMP	Bone Morphogenetic Protein
CAM	Cellular Adhesion Molecule
ECM	Extracellular Matrix
MMP2	Matrix Metalloproteinase-2
MMP8	Matrix Metalloproteinase-8
P1	1st Generation Piezotome®
P2	2nd Generation Piezotome®
qRT-PCR	Real-Time Reverse Transcriptase Polymerase Chain Reaction
R	High Speed Rotary Instrumentation
ROI	Region of Interest
S	Sham Surgery Control
TNF-α	Tumor Necrosis Factor-α
μCT	Micro-computed Tomography

PART I:

GENETIC EXPRESSION PROFILES FOLLOWING *IN VIVO* BONE INSTRUMENTATION WITH PIEZOTOME® ULTRASONIC SURGICAL UNITS

Abstract

The aim of this study is to evaluate differences in the genetic expression following the use of piezoelectric and rotary instrumentation for osteotomy preparation. Fourteen Sprague-Dawley rats underwent bilateral tibial osteotomies (n=28) prepared in a randomized split-leg design using either high speed rotary (R), 1st Generation Piezotome® (P1), or 2nd Generation Piezotome® (P2) instrumentation. Sham surgeries (S) served as controls. At 1 week, tibiae (n=12) were resected and processed for qRT-PCR array analysis. Osteotomies were also subject to immunohistochemistry for MMP2, MMP8, and TNF-α at 1 week and 3 weeks (n=8 each week). At 1 week, expression of 11 and 18 genes important in bone healing were significantly ($p<0.05$) decreased following P1 and P2 instrumentation, respectively, relative to S. Qualitative evaluation of immunohistochemistry confirmed cell positivity within the healing tissues. Variations in gene expression important to osseous wound healing suggest differences in healing rates due to surgical modality.

INTRODUCTION

Piezoelectric surgical units have been used in a variety of surgical treatments, including lateral window sinus lift techniques (Sohn et al., 2009; Vercellotti, De Paoli, & Nevins, 2001; Wallace et al., 2007), autogenous bone grafting (Happe, 2007; Sohn et al., 2007; Stubinger et al., 2006), implant site preparation (Preti et al., 2007), osteotomy close to nerves (Bovi et al., 2010; Geha et al., 2006), extractions (Degerliyurt et al., 2009; Grenga & Bovi, 2004), periodontal surgery (Vercellotti & Pollack, 2006), and distraction osteogenesis (Gonzalez-Garcia et al., 2008; Lee, Ahn, & Sohn, 2007). While the use of piezoelectric surgical units in dental applications has increased in recent history, little is known regarding the cellular and molecular responses of tissues to ultrasonic instrumentation.

Following insult, bone repair and/or regeneration occurs through the interaction of various bone cells, extracellular matrix components, and inorganic minerals. Bone repair undergoes three important phases: an acute inflammatory phase, a reparative phase, and a remodeling phase (Lieberman & Friendlaender, 2005). Endothelial damage as a result of injury activates the complement cascade, initiating the inflammatory phase of healing. Platelet aggregation also occurs during this phase and these platelets play a complex role in the release of growth factors and chemotactic agents, recruiting inflammatory cells such as leukocytes, lymphocytes, and macrophages. Platelets within the osseous defect form a hematoma which remodels to form a reparative granuloma, or callus. The reparative phase

of healing involves the formation of this fibroblastic callus to provide mechanical stability and serve as a framework for subsequent bone formation through the function of osteoblasts and chondroblasts. Finally, the remodeling phase occurs with the continued maturation of the bone over time through coordinated efforts by both osteoclasts and osteoblasts.

All of these events governing bone healing are coordinated by a number of biological processes (Ai-Aql et al., 2008; Einhorn, 1998; Lieberman & Friendlaender, 2005). These processes directing bone repair are tightly regulated by multiple factors, including proinflammatory cytokines, members of the transforming growth factor-β (TGF-β) superfamily, and angiogenic factors. Each of these groups has biological activity, including the promotion of overlapping biological processes and the orchestration of different interactions between differing cell populations. Inflammatory cytokines, including interleukin-1 and -6 (IL-1 and IL-6) and tumor necrosis factor-α (TNF-α), are expressed early in the *inflammatory phase* of bone healing and are predominantly secreted by macrophages and other inflammatory cells at the site of tissue injury. These cytokines serve as important factors in the initiation of the repair cascade, the recruitment of additional inflammatory cells, the deposition of extracellular matrix, and the stimulation of angiogenesis. Mesenchymal stem cells are subsequently recruited by TNF-α and induced to differentiate into chondrogenic or osteogenic cells by members of the TGF-β superfamily, including bone morphogenetic proteins (BMPs). A number of BMPs play important roles during this *reparative phase*, including BMP-2, BMP-4, and BMP-6, which serve to further direct extracellular matrix deposition and bone formation through the differentiation of osteoprogenitor cells. Expression of other angiogenic factors, such as vascular endothelial growth factors (VEGFs) and angiopoietins, are also upregulated during the *reparative phase*.

IL-1, TNF-α, and various BMPs are again upregulated during the *remodeling phase* in the demineralization of immature lamellar bone and subsequent remineralization to more mature woven bone. How these processes are affected by piezoelectric instrumentation is not completely known. Given the increased use of these instruments in clinical applications, it is important to understand the impact of ultrasonic instrumentation on osseous healing.

The purpose of this present study is to compare the genetic response of bone to piezoelectric surgical and traditional high speed rotary instrumentation in a rat tibia model. We hypothesize that the tissue regenerative response of bone to first- and second-generation piezoelectric units is equivalent or better than rotary instrumentation. We also hypothesize that there will be no difference in response to units with different power output capacities.

MATERIALS AND METHODS

Surgical Procedures

All experimental procedures followed a protocol approved by the Institutional Animal Care and Use Committee at The University of North Carolina at Chapel Hill. Fourteen male Sprague-Dawley rats (Charles River Laboratories International, Inc., Wilmington, MA) weighing approximately 250-300g were used for the study for a total of 28 tibiae. Rats were anesthetized with an intraperitoneal injection of ketamine/xylazine and the surgical sites shaved and disinfected with Betadine®. An incision was made along the medial aspect of each tibia. The overlying muscle was gently separated and the periosteum elevated. Using a randomized approach, a 6mm vertical osteotomy (n = 7 tibiae per treatment group) was prepared through the cortical bone in the medial aspect of each tibia using copious saline irrigation and either (1) the BS1 insert (Satelec Acteon, Merignac, France) mounted on the Piezotome® (Acteon) surgical unit (P1 group), (2) the BS1 insert mounted on the Implant Center 2 (Piezotome® 2, Acteon) surgical unit (P2 group), or (3) a ¼ round bur (Brassler USA, Savannah, GA) with high speed rotary instrumentation (Implant Center 2, Acteon) (R group). The power and irrigation settings were as follows: P1: Mode 1, 50 mL/min irrigation; P2: Mode D1, 60 mL/min irrigation; and R: 200,000 revolutions per minute, 60 mL/min irrigation. Surgical sham control surgeries (S group) (n = 7 tibiae) consisted of tissue elevation to expose bone for 3-5 minutes (the approximate time for osteotomy preparation). Following surgery, the periosteal/muscle tissues were sutured using 5-0 chromic gut followed by closing of flaps with 4-0 silk suture.

Rats were euthanized by CO_2 inhalation at either 1 week (n = 20 tibiae) or 3 weeks (n = 8 tibiae) after surgery. For tibias undergoing genetic analysis, residual muscle or soft tissues were carefully removed and the limbs resected at the level of articulation, snap frozen in liquid nitrogen, and stored at -80°C. For immunohistochemistry, postmortem cardiac perfusion fixation was completed using 10% neutral buffered formalin (NBF) and tibias were isolated at the level of articulation, fixed in 10% NBF for 48 hours, rinsed in phosphate buffered saline (PBS), and stored in 70% ethanol at 4°C.

RNA Isolation, Real-Time Reverse Transcriptase PCR

Tibias were homogenized in liquid nitrogen using a mortar and pestle, total RNA extracted using Trizol (Invitrogen, Carlsbad, CA) and further purified using the RNeasy Mini Kit (Qiagen, Germantown, MD) according to manufacturer's instructions. RNA integrity was assessed using a NanoDrop ND-1000 spectrophotometer (NanoDrop Technologies, Wilmington, DE) and the 2100 Bioanalyzer (Agilent Technologies, Santa Clara, CA). For each sample, synthesis of cDNA was completed from 1 μg of total RNA using the Omniscript Kit (Qiagen) and random decamer primers (Applied Biosystems/Ambion, Austin, TX) according to manufacturer's instructions. qRT-PCR was performed using the Rat Osteogenesis RT^2 Profiler™ PCR Array (SABiosciences, Frederick, MD) on an ABI PRISM® 7500 Real-Time PCR Thermal Cycler (Applied Biosystems, Foster City, CA) according to manufacturer's instructions. Cycling conditions included an initial cycle of 2 min at 50°C and 10 min at 95°C, followed by a 40 cycles of 15 sec at 95 C ° and 1 min at 60°C. Each Rat Osteogenesis RT^2 Profiler™ PCR Array contained 84 wells with primers for

different genes related to skeletal development, bone mineral metabolism, cell growth and differentiation, extracellular matrix proteins, transcription factors and regulators, and cell adhesion molecules. RT^2 Profiler™ PCR Array Data Analysis software (SABiosciences) was used to calculate threshold cycle (Ct) values. Data was analyzed using the $2^{-\Delta\Delta Ct}$ method and results reported as fold change (Livak & Schmittgen, 2001). Differentially expressed genes were subsequently classified by Gene Ontology terms.

Immunohistochemistry

Automated IHC was performed using the DAKO Autostainer Plus system (DAKO, Carpinteria, CA) at room temperature. Tissues fixed in 10% NBF were rinsed in PBS and demineralized by immersion in Immunocal (Decal Chemical Corporation, Tallman, NY) for 2 weeks at room temperature. Complete decalcification was confirmed by lack of radiopacity using microCT scans (Skyscan, Aartselaar, Belgium). Tissues were processed with routine ethanol dehydrations, xylene clearing, and paraffin infiltrations. Specimens were axially sectioned at a thickness of 5 μm onto subbed glass slides, deparaffinized, rehydrated using graded ethanols and finally with distilled water. After rinsing in running water, slides were placed in Tris buffer. When required, antibody retrieval was completed using Pascal retrieval unit (DAKO) and Target retrieval solution, pH 6.0 (DAKO). Sections were exposed to the dual endogenous enzyme block (DAKO) for 10 minutes, rinsed with Tris, and blocked with serum free protein (DAKO) for 15 minutes. Primary antibody dilutions for MM2, MMP8, and TNF-α (Abcam Incorporated, Cambridge, MA) were 1:50, 1:50, and 1:800, respectively. After 60 minutes, anti-rabbit (MMP8, TNF-α) or anti-mouse

(MMP2) secondary antibody (Envision+, DAKO) was applied for 45 minutes followed by DAB+ chromagen (DAKO) for an additional 10 minutes. The slides were counterstained with hematoxylin and examined by light microscopy. The presence and location of staining for the different antibodies was described by a blinded examiner.

Statistics

Statistical analyses of gene expression group differences were identified using the web-based RT^2 Profiler™ PCR Array Data Analysis program (SABiosciences). Alpha values ≤ 0.05 were used for all tests to indicate statistical significance.

RESULTS

Real-Time Reverse Transcriptase PCR

A list of the genes with statistically significant differential expression levels is present in Table 1 with corresponding representative biological process Gene Ontology terms. Of the 84 genes examined, 28 had significant differences ($p<0.05$) in expression when comparing P1 and P2 to S (Table 2) while 19 had significant differences ($p<0.05$) in expression when compared to R (Table 3). Expression of genes involved in a number of biological processes related to both osseous wound healing and cellular events important in wound healing were diminished relative to S (Figure 1) and R groups (Figure 2).

When compared to S (Table 2), decreased expression of 3 genes (*Comp, Smad3, Vegfa*) and increased expression of 1 gene (*Col3a1*) was noted in the R group. In comparison, the expression of 18 (*Bmpr1a, Col4a1, Col5a1, Col6a1, Col12a1, Col14a1, Fgfr1, Fn1, Gdf10, Igf1, Itgav, Itgb1, Mmp2, Scarb1, Smad1, Tgfb3, Tnf, Tuft1*) and 11 (*Bmp6, Bmp7, Bmpr1a, Col14a1, Gdf10, Igf1r, Itga3, Itgam, Mmp8, Smad1, Tuft1*) genes were significantly decreased in the P1 and P2 groups, respectively, relative to S. No genes were significantly upregulated following P1 or P2 instrumentation relative to S.

When R was used as a reference group, 16 genes (*Anxa5, Bgn, Bmp4, Col3a1, Col4a1, Col5a1, Col6a1, Col12a1, Col14a1, Igf1, Itgav, Itgb1, Msx1, Scarb1, Smad1,*

Tgfbr3) had statistically significant decreases in expression following instrumentation with P1 compared to 4 genes (*Col14a1, Itgam, Tgfb1, Tgfbr3*) with statistically significant lower expression levels following use of the P2 unit. There was a statistically significant upregulation of 1 gene (*Egf*) following osteotomy preparation with P1, but not with P2 preparation.

Immunohistochemistry

MMP2. *Sham surgeries* At 1 week (Figure 3a) post-surgery, MMP2-positive cells were present lining the inner cortical bone with the exception of the cells immediately adjacent to the surgical site. Immunopositive cells were present lining the Haversian canals of the bone at the interface between osteoblasts and the bony matrix. A notable gradient of immunopositive cells was identified, with a greater number of immunopositive cells present in the outer aspect of the bony bridge relative to the inner aspect. Osteocytes were negative. Uniform bone marrow immunopositivity was present with megakaryocytes in the marrow immunopositive for MMP2. Immunoreactivity was present in the fibroblasts of the soft tissue overlying the apparent S site. Similar findings were noted at 3 weeks (Figure 3b) post-surgery with the exception of the presence of immunoreactive cells lining the inner aspect of the S sites, a finding that was not present at 1 week. Furthermore, the amount of reactive cells at 3 weeks had decreased substantially relative to the 1 week samples. *Treatment groups* Similar patterns of reactivity were noted at 1 (Figure 3a) and 3 weeks (Figure 3b) relative to S controls. Decreased reactivity appeared present in the overlying soft tissue fibroblasts of P1 and P2 relative to S at 1 and 3 weeks. At 3 weeks, decreased reactivity of R

was also noted relative to S. No difference in reactivity was evident in osteotomy sites relative to the bone immediately adjacent to the osteotomy defect. Minimal differences in reactivity were noted between the three treatment groups at 1 and 3 weeks.

MMP8. *Sham surgeries* At 1 week (Figure 4a) and 3 weeks (Figure 4b) post-surgery, MMP8-positive cells had a presentation remarkably similar to the MMP2-positive cells. MMP8 cells circumferentially lined the inner cortical bone, including the cells immediately beneath the surgical site. In the surgical site, positive cells were present lining the Haversian canals of the bony bridge spanning the bone with a greater number of immunopositive cells present in the outer aspect of the bone relative to the inner aspect. Osteocytes were negative. Uniform bone marrow immunopositivity was present with a weaker reactivity relative to the MMP2- and TNF-α-positive cells. Unlike MMP2 immunostaining, no megakaryocyte reactivity was identified within the marrow space or in other surrounding tissues. Osteoblasts associated with the overlying periosteum were immunoreactive. Additionally, with the exception of P1 and P2 at 3 weeks, there was slightly less reactivity identified in the overlying soft tissue fibroblasts relative to the MMP2-positive cells. *Treatment groups* Similar findings were noted at 1 (Figure 4a) and 3 weeks (Figure 4b) relative to S controls with the exception of the absence of reactivity of the cells lining the osteotomy defect. While there were no reactive cells lining the stromal aspect of the newly formed bony bridge, a gradient of reactive cells within the newly formed bony bridge was identified similar to the S specimens. Decreased reactivity that appeared present in the overlying soft tissues of P1 and P2 relative to S at 1 week was no longer apparent at 3 weeks. At 3 weeks, decreased reactivity of R was noted relative to S.

TNF-α. *Sham surgeries* At 1 week post-surgery (Figure 5a), TNF-α-positive cells had a presentation similar to the MMP2- and MMP8-positive cells. Cells expressing TNF-α lined the inner cortical bone circumferentially. Similar to the MMP2 and MMP8 staining patterns, a gradient of cell reactivity was present in the Haversian canals adjacent to the surgical site with increased cell reactivity present on the outer aspect of the bony bridge relative to the inner aspect. Osteocytes were negative. Uniform non-specific bone marrow positivity was present. Very few fibroblasts in the overlying soft tissues were positive for TNF-α. Minimal differences in reactivity were noted at 3 weeks post-surgery (Figure 5b). *Treatment groups* Similar reactivity patterns were noted at 1 and 3 weeks relative to S controls. Decreased fibroblastic reactivity was noted in all three treatment groups at 1 week relative to S controls, but not at 3 weeks. Bone marrow reactivity was visibly more significant in the treatment groups relative to S, with no notable differences in reactivity present among the different treatment groups.

Table 1. Gene Table. **Genes with significant differential expression in mechanical osteotomies using the different surgical modalities at 1 week post-surgery.**		
Gene Abbreviation	**Gene Name**	**Gene Ontology Term***
Cell-Matrix Adhesion Proteins		
Itga3	Integrin, alpha 3	Cell adhesion
Itgam	Integrin, alpha M	Cell adhesion
Itgav	Integrin, alpha V	Cell adhesion
Itgb1	Integrin, beta 1	Cell adhesion
Cytokines		
Tnf	Tumor necrosis factor	Inflammatory response
ECM Proteases		
Mmp2	Matrix metallopeptidase 2	Tissue remodeling
Mmp8	Matrix metallopeptidase 8	Proteolysis
Growth Factors		
Bmp4	Bone morphogenetic protein 4	Osteoblast differentiation
Bmp6	Bone morphogenetic protein 6	Osteoblast differentiation
Bmp7	Bone morphogenetic protein 7	Positive regulation of osteoblast differentiation
Gdf10	Growth differentiation factor 10	Regulation of ossification
Igf1	Insulin-like growth factor 1	Positive regulation of osteoblast differentiation
Tgfb1	Transforming growth factor, beta 1	Wound healing
Tgfb3	Transforming growth factor, beta 3	Positive regulation of bone mineralization
Vegfa	Vascular endothelial growth factor A	Angiogenesis
Extracellular Matrix Proteins		
Bgn	Biglycan	Blood vessel remodeling
Col3a1	Collagen, type III, alpha 1	Collagen fibril organization
Col4a1	Collagen, type IV, alpha 1	Epithelial cell differentiation
Col5a1	Collagen, type V, alpha 1	Collagen fibril organization
Col6a1	Collagen, type VI, alpha 1	Protein heterotrimerization
Col12a1	Collagen, type XII, alpha 1	Cell adhesion
Col14a1	Collagen, type XIV, alpha 1	Cell adhesion
Comp	Cartilage oligomeric matrix protein	Extracellular matrix organization
Fn1	Fibronectin 1	Cell adhesion
Tuft1	Tuftelin 1	n/a
Receptors		
Bmpr1a	Bone morphogenetic protein receptor, type IA	Positive regulation of bone mineralization
Fgfr1	Fibroblast growth factor receptor 1	Chondrocyte development
Igf1r	Insulin-like growth factor 1 receptor	Positive regulation of cell migration
Scarb1	Scavenger receptor class B, member 1	Blood vessel endothelial cell migration
Tgfbr3	Transforming growth factor, beta receptor III	BMP signaling pathway
Transcription Factors & Signaling Molecules		
Anxa5	Annexin A5	Response to organic substance
Msx1	Msh homeobox 1	BMP signaling pathway
Smad1	SMAD family member 1	BMP signaling pathway
Smad3	SMAD family member 3	Osteoblast development

*Only one biologic process gene ontology term is presented for each gene.

Table 2. Gene Downregulation/Upregulation Following 1st Generation Piezotome®, 2nd Generation Piezotome®, or High Speed Rotary Instrumentation. **Gene expression as fold regulation following mechanical osteotomies using R, P1, or P2 instrumentation compared to S at 1 week post-surgery.**

	Rotary Instrumentation (R)		1st Generation Piezotome® (P1)		2nd Generation Piezotome® (P2)	
	Fold Regulation	p-value	Fold Regulation	p-value	Fold Regulation	p-value
Cell-Matrix Adhesion Proteins						
Itga3	-1.2357	0.11056	-1.5171	0.12906	-2.0458*	0.01756
Itgam	-1.0757	0.67749	-1.5670	0.22292	-1.8912*	0.01131
Itgav	1.1132	0.27933	-1.6756*	0.02300	-1.2506	0.32323
Itgb1	1.0410	0.66141	-1.3864*	0.02511	-1.2564	0.36985
Cytokines						
Tnf	1.0172	0.76198	-1.4123*	0.01494	1.0872	0.63831
ECM Proteases						
Mmp2	-1.0295	0.98403	-1.9972*	0.01874	-1.5011	0.51686
Mmp8	-1.3398	0.19011	-1.5598	0.33539	-2.0936*	0.01208
Growth Factors						
Bmp6	-1.1292	0.50375	-1.3361	0.14413	-1.6163*	0.04416
Bmp7	-1.5248	0.17865	-1.4025	0.11984	-2.5245*	0.01969
Gdf10	-1.2912	0.21974	-1.5670*	0.03276	-1.8566†	0.00964
Igf1	1.0604	0.61550	-1.5889†	0.00459	-1.3189	0.27463
Tgfb3	1.0362	0.73031	-1.1931*	0.01133	-1.1562	0.76492
Vegfa	-1.3967*	0.02633	1.0084	0.82389	-1.2193	0.13801
Extracellular Matrix Proteins						
Col3a1	1.3177†	0.00783	-1.4756	0.06018	-1.0112	0.98055
Col4a1	1.0291	0.78751	-1.7068*	0.01329	-1.4070	0.08380
Col5a1	1.0629	0.62551	-1.4287*	0.03941	-1.1402	0.72795
Col6a1	1.0654	0.48652	-1.9070†	0.00055	-1.5256	0.11172
Col12a1	-1.0319	0.78660	-1.6756†	0.00738	-1.1669	0.47909
Col14a1	1.3146	0.13309	-2.3316*	0.02379	-1.3654†	0.00219
Comp	-2.0401*	0.03725	1.0177	0.89054	-1.1887	0.58171
Fn1	-1.0512	0.87389	-1.6563†	0.00528	-1.4006	0.11122
Tuft1	-1.2243	0.37667	-1.9697*	0.01005	-2.1876†	0.00829
Receptors						
Bmpr1a	-1.2019	0.15650	-1.3299*	0.02704	-1.4499*	0.02509
Fgfr1	-1.1909	0.16222	-1.4123*	0.04724	-1.4567	0.14212
Igf1r	-1.0683	0.75299	-1.4621	0.18624	-1.7045*	0.01623
Scarb1	1.0852	0.15542	-1.3896*	0.02236	-1.2420	0.22783
Transcription Factors & Signaling Molecules						
Smad1	-1.1991	0.20281	-1.8251†	0.00521	-1.8226*	0.01494
Smad3	-1.4560*	0.03014	-1.2097	0.15566	-1.4433	0.07028

*Significant difference between R, P1, or P2 instrumentation and S controls at $p < 0.05$.

†Significant difference between R, P1, or P2 instrumentation and S controls at $p < 0.01$.

Table 3. Gene Downregulation/Upregulation Following 1st Generation Piezotome®, 2nd Generation Piezotome®, or High Speed Rotary Instrumentation. **Statistically significant differential gene expression following mechanical osteotomies using R, P1, or P2 instrumentation compared to S at 1 week post-surgery.**

Rotary Instrumentation (R)		**1st Generation Piezotome® (P1)**		**2nd Generation Piezotome® (P2)**	
downregulation	upregulation	downregulation	upregulation	downregulation	upregulation
Comp	*Col13a1*	*Bmpr1a*		*Bmp6*	
Smad3		*Col4a1*		*Bmp7*	
Vegfa		*Col5a1*		*Bmpr1a*	
		Col6a1		*Col14a1*	
		Col12a1		*Gdf10*	
		Col14a1		*Igf1r*	
		Fgfr1		*Itga3*	
		Fn1		*Itgam*	
		Gdf10		*Mmp8*	
		Igf1		*Smad1*	
		Itgav		*Tuft1*	
		Itgb1			
		Mmp2			
		Scarb1			
		Smad1			
		Tgfb3			
		Tnf			
		Tuft1			

Table 4. Gene Expression Fold Regulations Following 1st Generation Piezotome® or 2nd Generation Piezotome® Instrumentation. **Gene expression as fold regulation following mechanical osteotomies using P1 or P2 instrumentation compared to R at 1 week post-surgery.**

	1st Generation Piezotome® (P1)		2nd Generation Piezotome® (P2)	
	Fold Regulation	p-value	Fold Regulation	p-value
Cell Matrix Adhesion Proteins				
Itgam	-1.4567	0.32708	-1.7581*	0.02271
Itgav	-1.8652†	0.00360	-1.3922	0.11408
Itgb1	-1.4433†	0.00730	-1.3080	0.26900
Growth Factors				
Bmp4	-1.5220*	0.03051	-1.6178	0.09856
Egf	2.4691†	0.00774	1.2306	0.24125
Igf1	-1.6849*	0.01960	-1.3986	0.22123
Tgfb1	-1.5150	0.07687	-1.6943*	0.04703
Extracellular Matrix Proteins				
Bgn	-1.3497*	0.03881	-1.2547	0.50658
Col3a1	-1.9444†	0.00938	-1.3324	0.08576
Col4a1	-1.7565*	0.01171	-1.4479	0.06803
Col5a1	-1.5185†	0.00121	-1.2120	0.54121
Col6a1	-2.0317†	0.00261	-1.6253	0.08485
Col12a1	-1.6238†	0.00785	-1.1308	0.58432
Col14a1	-3.0652*	0.01979	-1.7950*	0.02776
Receptors				
Scarb1	-1.5080*	0.01405	-1.3479	0.11515
Tgfbr3	-1.5397*	0.02080	-1.5270*	0.04095
Transcription Factors & Signaling Molecules				
Anxa5	-1.5256*	0.02040	-1.3510	0.23996
Msx1	-1.5115*	0.02193	-1.6103	0.11687
Smad1	-1.5220*	0.02419	-1.5199	0.06147

*Significant difference between P1 or P2 and R instrumentation groups at $p < 0.05$.

†Significant difference between P1 or P2 and R instrumentation groups at $p < 0.01$.

Table 5. Gene Downregulation/Upregulation Following 1st Generation Piezotome® or 2nd Generation Piezotome® Instrumentation. **Statistically significant differential gene expression following mechanical osteotomies using P1 or P2 instrumentation compared to R at 1 week post-surgery.**

1st Generation Piezotome® (P1)		**2nd Generation Piezotome® (P2)**	
downregulation	upregulation	downregulation	upregulation
Anxa5	*Egf*	*Col14a1*	
Bgn		*Itgam*	
Bmp4		*Tgfb1*	
Col3a1		*Tgfbr3*	
Col4a1			
Col5a1			
Col6a1			
Col12a1			
Col14a1			
Igf1			
Itgav			
Itgb1			
Msx1			
Scarb1			
Smad1			
Tgfbr3			

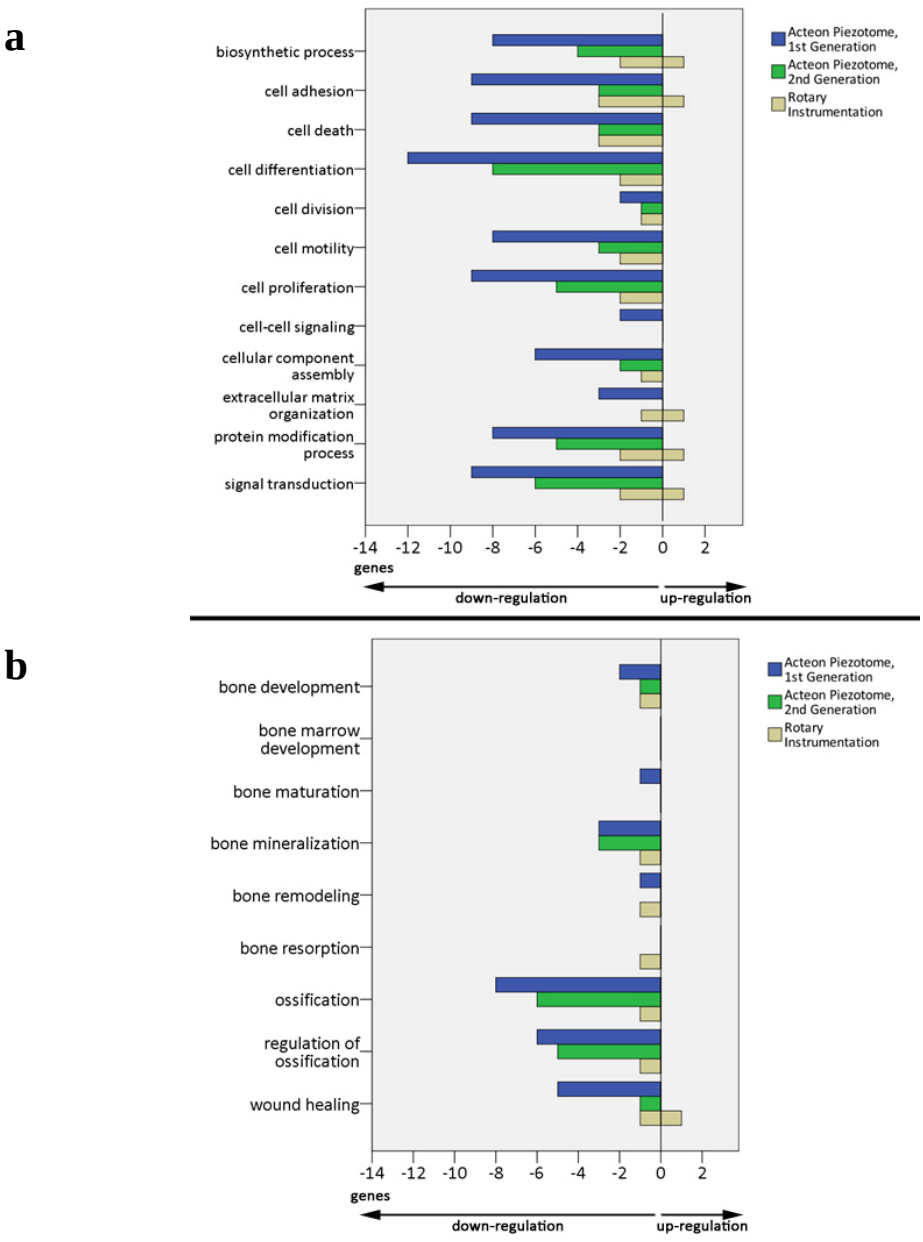

Figure 1. Downregulation/Upregulation of Genes Important in Cellular Processes and Osseous Wound Healing following 1st Generation Piezotome®, 2nd Generation Piezotome®, or High Speed Rotary Instrumentation. Numbers of genes relevant to (a) cellular processes or (b) osseous wound healing, as classified by Gene Ontology, up- or down-regulated following osteotomy creation with P1 or P2 instrumentation or with R instrumentation relative to S controls.

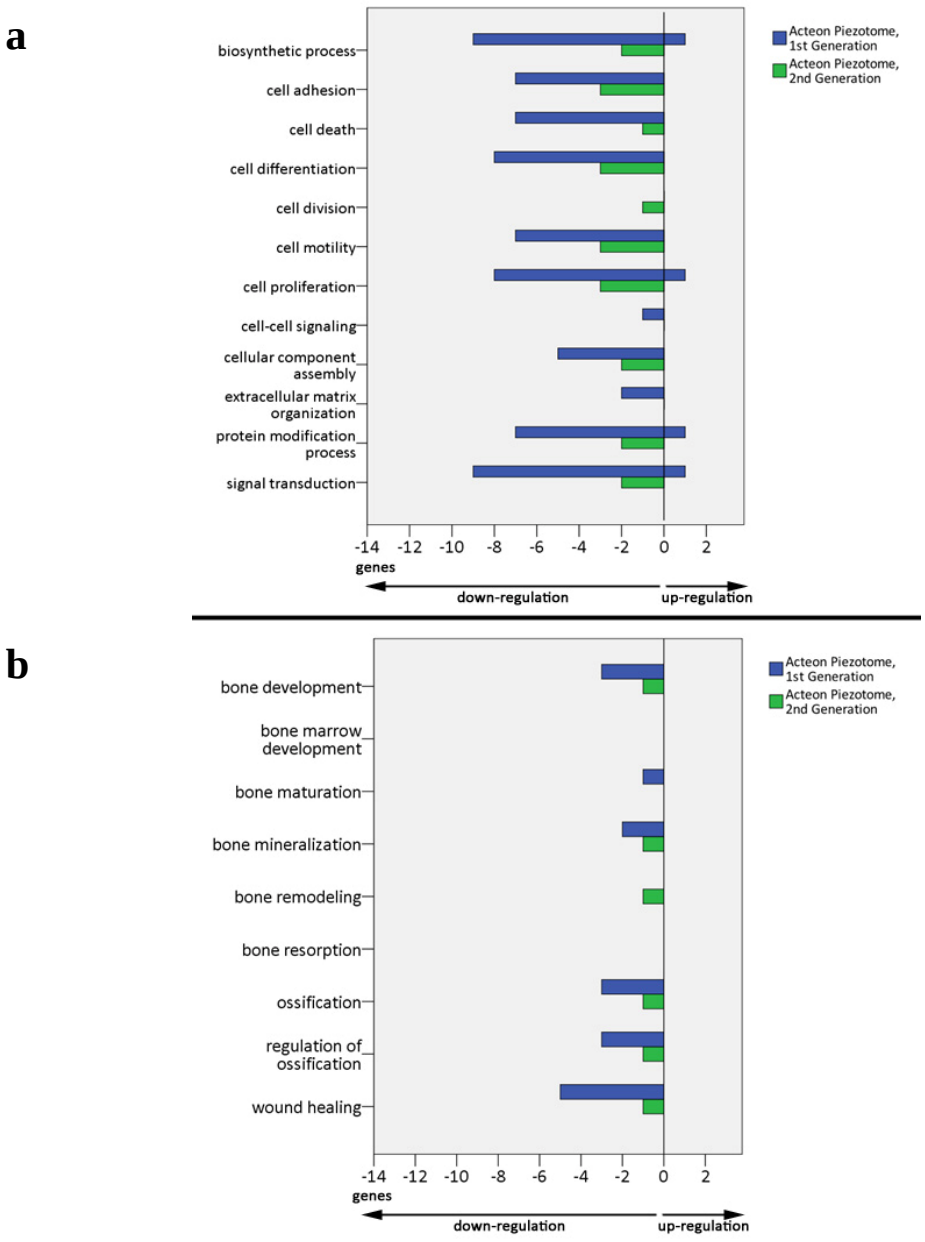

Figure 2. Downregulation/Upregulation of Genes Important in Cellular Processes and Osseous Wound Healing following 1st Generation Piezotome® or 2nd Generation Piezotome® Instrumentation. Numbers of genes relevant to (a) cellular processes or (b) osseous wound healing, as classified by Gene Ontology, up- or down-regulated following osteotomy creation with P1 or P2 instrumentation relative to R instrumentation.

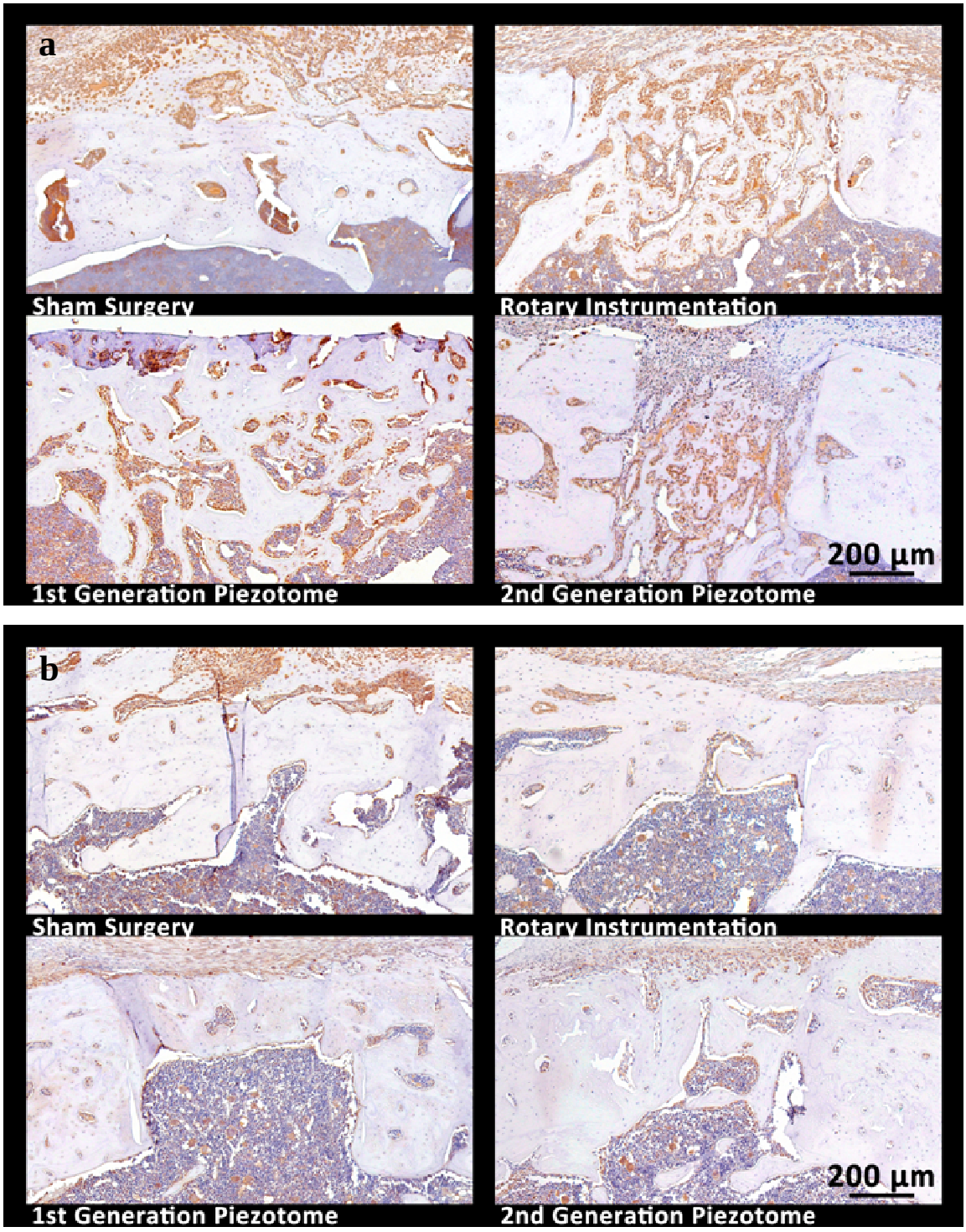

Figure 3. MMP2 Immunohistochemistry at 1 and 3 Weeks Post-Surgery.

Immunohistochemistry staining with anti-MMP2 antibodies at 1 week (Figure 3a) and 3 weeks (Figure 3b) post-surgery for the different treatment modalities and S controls.

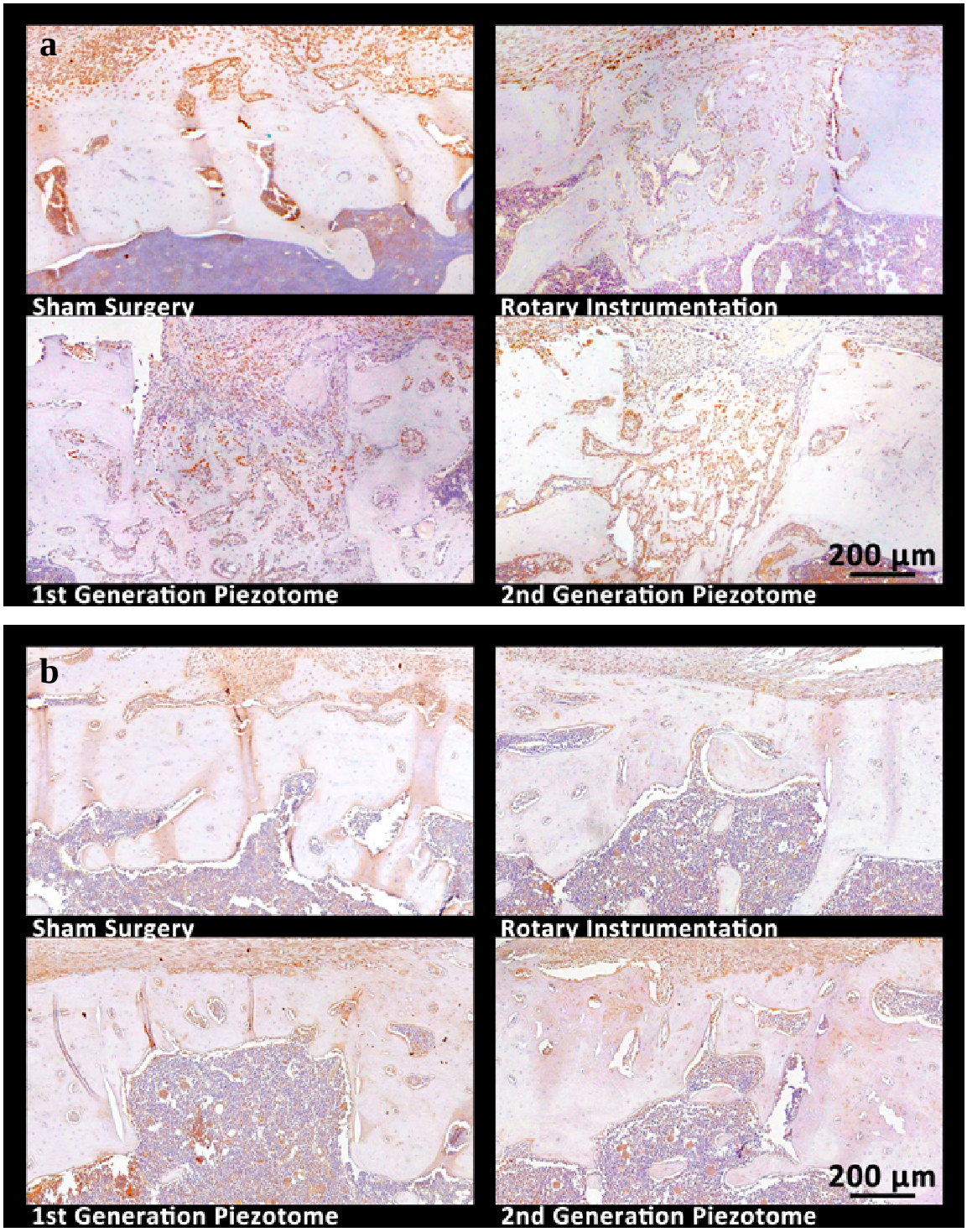

Figure 4. MMP8 Immunohistochemistry at 1 and 3 Weeks Post-Surgery.

Immunohistochemistry staining with anti-MMP8 antibodies at 1 week (Figure 4a) and 3 weeks (Figure 4b) post-surgery for the different treatment modalities and S controls.

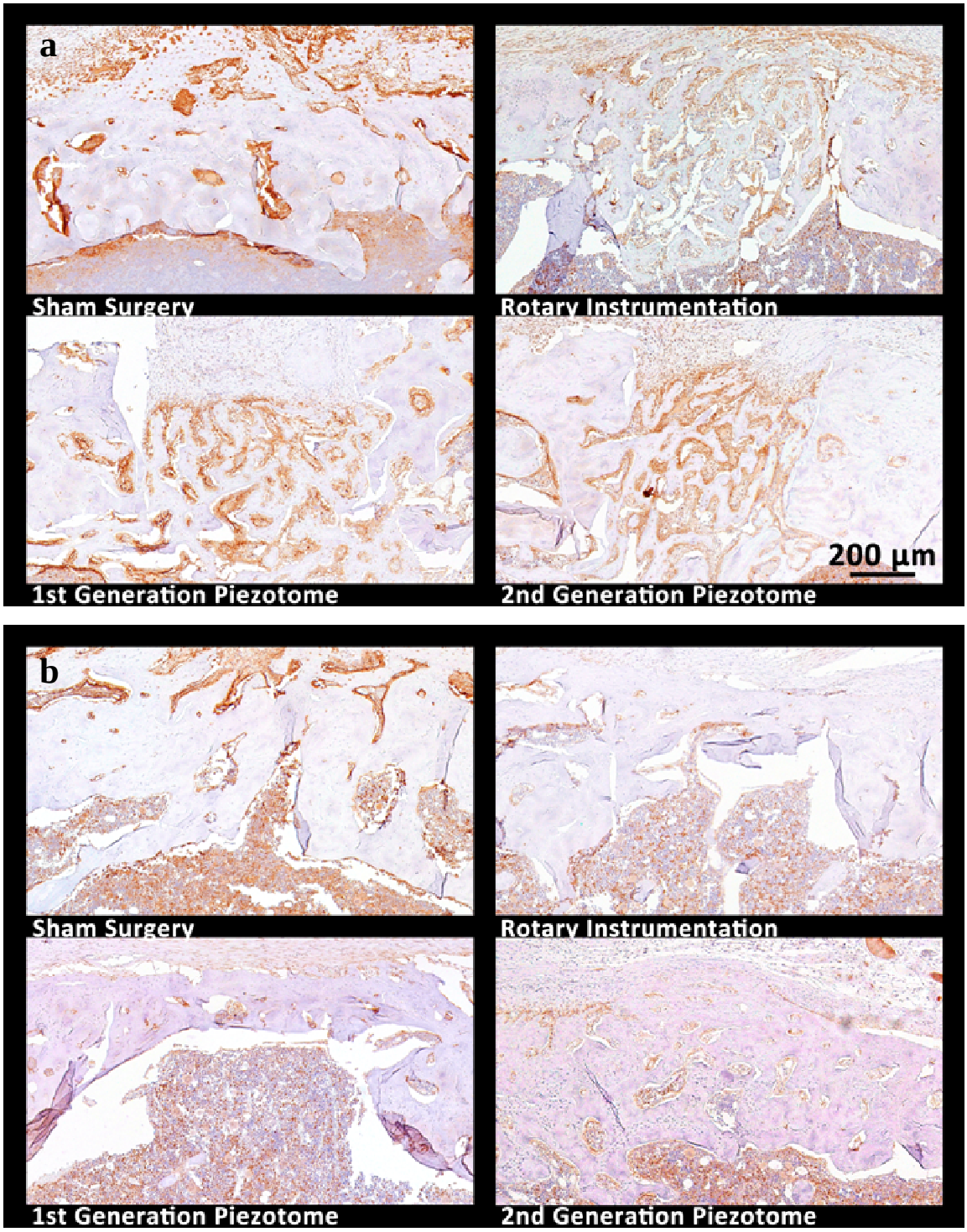

Figure 5. TNF-α Immunohistochemistry at 1 and 3 Weeks Post-Surgery.

Immunohistochemistry staining with anti-TNF-α antibodies at 1 week (Figure 5a) and 3 weeks (Figure 5b) post-surgery for the different treatment modalities and S controls.

DISCUSSION

Numerous studies have documented the clinical effectiveness of piezoelectric surgery (Bovi et al., 2010; Degerliyurt et al., 2009; Geha et al., 2006; Gonzalez-Garcia et al., 2008; Grenga & Bovi, 2004; Happe, 2007; Lee, Ahn, & Sohn, 2007; Preti et al., 2007; Sohn et al., 2007; Sohn et al., 2009; Stubinger et al., 2006; Vercellotti, De Paoli, & Nevins, 2001; Vercellotti & Pollack, 2006; Wallace et al., 2007) but few have documented the cellular and molecular responses of bone to this form of instrumentation. We compared the 1 week healing of osteotomies prepared using conventional rotary and piezoelectric instrumentation to surgical sham controls using a focused osteogenesis PCR array. We also evaluated the osseous responses to two unique piezoelectric units and in doing so we were able to compare the effects of different power output capacities. Overall the results of our study demonstrate that gene expression linked to bone remodeling at sites prepared by rotary instrumentation requires a more robust genetic response relative to 1st and even the more powerful 2nd generation Piezotome® unit. This indicates that gene activity associated with bone regeneration and remodeling at sites prepared by ultrasonic instrumentation may be activated at an earlier time point and/or does not require a prolonged expression pattern to support osseous healing as seen using rotary instrumentation. Indeed, μCT analysis of week 3 osteotomies indentified statistically significant increases in percent bone fill and bone mineral density along the peripheral aspect of the osteotomies prepared by P2 compared to R

suggesting differences in bone maturation rates (Part II). Alternatively, the piezoelectric surgical tip itself and/or the energy imparted on it during osteotomy preparation is more biologically favorable relative to a round rotating bur. To exclude the possibility of a dull bur contributing to osseous trauma, each osteotomy preparation using rotary instrumentation was performed using a fresh ¼ round bur. Taken together, this implies that the choice of surgical modality impacts osseous healing rates with piezoelectric instrumentation yielding lower levels of bone trauma compared to traditional rotary instrumentation.

Following injury, temporal gene expression patterns are determined by overlapping stages of tissue repair, largely recapitulating embryonic developmental processes (Gerstenfeld & Einhorn, 2003; Rundle et al., 2006). Trauma to endochondral bones leads to hematoma formation and inflammation resulting in upregulation of cytokine expression. Cartilage formation occurs, in which extracellular matrix, angiogenic, and morphogenetic protein expression is upregulated. These various proteins continue to undergo upregulation during primary bone formation which is coupled with cartilage resorption, resulting in further cytokine upregulation. Subsequently, the bone undergoes continued remodeling processes (Gerstenfeld & Einhorn, 2003). The expression of proinflammatory cytokines and matrix proteins in mice peaks within 24 hours of fracture, declining to very low levels approximately 3 days after injury. Sequential peaks in the expression of genes important in the chondrogenic and osteogenic phases of remodeling occur at day 7 and at days 14-21, respectively (Cho, Gerstenfeld, & Einhorn, 2002). At 7 days, our data indicate differences in gene expression resulting from differences in surgical modality. To the best of our knowledge, no literature has been published detailing the stages of osseous healing and temporal gene expression patterns following experimental tibial osteotomies.

At 1 week, the expression of several cellular adhesion molecules (CAMs) and extracellular matrix (ECM) proteins were significantly decreased ($p<0.05$) in the P1 or P2 groups relative to R and S reference groups. In osseous fracture repair, expression of several CAM and ECM genes has been identified 11 days post-fracture, likely corresponding with endochondral tissue development and/or osseous replacement and formation at this stage of healing (Rundle et al., 2006). Similarly, *Bmp4* expression following P1 instrumentation and *Tgfbr3* expression following P1 and P2 instrumentation are significantly diminished relative to R ($p<0.05$). *Bmp4* expression is upregulated during active osteogenesis, while the function of *Tgfbr3* expression involves protein binding (including GDF5, BMP-2, BMP-4, and BMP-7) important in the chondrogenic and osteogenic phases of healing (Cho et al., 2002; Kirkbride et al., 2008). Relative decreases in the expression of these proteins at this time point following piezoelectric instrumentation, while currently unexplained, may possibly be related and linked to accelerated healing and/or decreased trauma.

Immunohistochemistry was completed to confirm the translation of several genes (*Mmp2*, *Mmp8*, and *Tnf*) expressed among the three groups. Increased protein expression was qualitatively identified with immunohistochemistry at 1 week relative to 3 weeks, consistent with previously reported expression levels of TNF-α and MMP2, but contradictory with levels of MMP8 previously identified in osseous fracture healing at these times points (Gerstenfeld et al., 2003; Lehmann et al., 2005).

An interesting finding was the significant histological appearance of surface pitting of bone in the S group along areas where periosteal tissues were only reflected. Studies (Brownlow et al., 2000; Fickl et al., 2011; Lobene & Glickman, 1963; Wood et al., 1972) have indicated that reflection of periosteal tissues triggers significant bone remodeling

processes and it is likely that this process contributed to osseous healing and our findings. Nevertheless it is important to account for tissue activity due to periosteal reflection at the genetic and tissue level.

These findings, when examined in conjunction with the downstream μCT and histological findings described in Part II, provide further evidence that diminished levels of these factors following piezoelectric instrumentation may be due to an acceleration in wound healing and/or decreased trauma. Differences in the rates of healing will influence the gene expression patterns among the different treatment groups at any particular time. This may support the reduced mRNA levels of the CAMs and ECM at this time point. Conversely, it is possible that the different surgical modalities may have had different effects on peripheral osseous structures adjacent to the osteotomy, potentially influencing not only the rate of healing within the osteotomy site, but also the timing, duration, and degree of gene expression. Surgical modalities causing damage to peripheral osseous tissues or inducing peripheral bone resorption may necessitate increased gene expression levels to accommodate an increased need for healing. Indeed, it is likely that piezoelectric instrumentation results in fewer changes to adjacent bone which may help explain the reduced levels of *Bmp4* and *Tgfbr3* mRNA at 1 week. The effects of the different surgical modalities on peripheral osseous structures will be evaluated in Part II of this manuscript.

The biological bases for our observations are not completely understood, however additional factors such as post-treatment bone microstructure, vascularity, inflammatory response, and others may impact osseous healing.

CONCLUSIONS

Following osteotomy preparation with piezoelectric instrumentation, there are differential expression levels of genes important in osseous healing relative to high speed rotary insrumentation and surgical sham controls. Decreased mRNA levels of 18 genes after P1 instrumentation and 11 genes following P2 instrumentation were present when sham surgeries were used as a reference group. This differential expression pattern is hypothesized to be related to effects of the different surgical modalities on adjacent bone structure, including trauma, that may influence either the rate of the healing process or the amount of gene expression necessary for bone healing. Immunohistochemistry confirmed the expression of genes with differential expression levels, including MMP2, MMP8, and TNF-α. Their expression was localized to the defect areas and adjacent peripheral tissues with differences in expression levels present between 1 and 3 weeks. Additional research is necessary to evaluate and compare gene expression levels between the three different treatment modalities at all stages of the bone healing process, including at 24 hours (start of inflammatory phase), 72 hours (end of inflammatory phase), 7 days (peak of chondrogenic phase), and 14-21 days (peak of osteogenic phase). These will permit better conclusions to be drawn regarding differences in gene expression at different times during the healing process and their effect on the rate of healing.

REFERENCES

Ai-Aql, Z. S., Alagl, A. S., Graves, D. T., Gerstenfeld, L. C., & Einhorn, T. A. (2008) Molecular mechanisms controlling bone formation during fracture healing and distraction osteogenesis. *Journal of Dental Research* **87**: 107-118.

Bovi, M., Manni, A., Mavriqi, L., Bianco, G., & Celletti, R. (2010) The use of piezosurgery to mobilize the mandibular alveolar nerve followed immediately by implant insertion: a case series evaluating neurosensory disturbance. *The International Journal of Periodontics and Restorative Dentistry* **30**: 73-81.

Brownlow, H. C., Reed, A., Joyner, C., & Simpson, A. H. (2000) Anatomical effects of periosteal elevation. *Journal of Orthopaedic Research* **18**: 500-502.

Cho, T. J., Gerstenfeld, L. C., & Einhorn, T. A. (2002) Differential temporal expression of members of the transforming growth factor beta superfamily during murine fracture healing. *Journal of Bone and Mineral Research* **17**: 513-520.

Degerliyurt, K., Akar, V., Denizci, S., & Yucel, E. (2009) Bone lid technique with piezosurgery to preserve inferior alveolar nerve. *Oral Surgery, Oral Medicine, Oral Pathology, Oral Radiology, and Endodontics* **108**: e1-5.

Einhorn, T. A. (1998) The cell and molecular biology of fracture healing. *Clinical Orthopaedics and Related Research* **(355 Suppl)**: S7-21.

Fickl, S., Kebschull, M., Schupbach, P., Zuhr, O., Schlagenhauf, U., & Hurzeler, M. B. (2011) Bone loss after full-thickness and partial-thickness flap elevation. *Journal of Clinical Periodontology* **38**: 157-162.

Geha, H. J., Gleizal, A. M., Nimeskern, N. J., & Beziat, J. L. (2006) Sensitivity of the inferior lip and chin following mandibular bilateral sagittal split osteotomy using piezosurgery. *Plastic and Reconstructive Surgery* **118**: 1598-1607.

Gerstenfeld, L. C., Cho, T. J., Kon, T., Aizawa, T., Tsay, A., Fitch, J., Barnes, G. L., Graves, D. T., & Einhorn, T. A. (2003) Impaired fracture healing in the absence of TNF-alpha signaling: the role of TNF-alpha in endochondral cartilage resorption. *Journal of Bone and Mineral Research* **18**: 1584-1592.

Gerstenfeld, L. C., & Einhorn, T. A. (2003) Developmental aspects of fracture healing and the use of pharmacological agents to alter healing. *Journal of Musculoskeletal and Neuronal Interactions* **3**: 297-303; discussion 320-1.

Gonzalez-Garcia, A., Diniz-Freitas, M., Somoza-Martin, M., & Garcia-Garcia, A. (2008) Piezoelectric and conventional osteotomy in alveolar distraction osteogenesis in a series of 17 patients. *The International Journal of Oral and Maxillofacial Implants* **23**: 891-896.

Grenga, V., & Bovi, M. (2004) Piezoelectric surgery for exposure of palatally impacted canines. *Journal of Clinical Orthodontics* **38**: 446-448.

Happe, A. (2007) Use of a piezoelectric surgical device to harvest bone grafts from the mandibular ramus: report of 40 cases. *The International Journal of Periodontics & Restorative Dentistry* **27**: 241-249.

Kirkbride, K. C., Townsend, T. A., Bruinsma, M. W., Barnett, J. V., & Blobe, G. C. (2008) Bone morphogenetic proteins signal through the transforming growth factor-beta type III receptor. *The Journal of Biological Chemistry* **283**: 7628-7637.

Lee, H. J., Ahn, M. R., & Sohn, D. S. (2007) Piezoelectric distraction osteogenesis in the atrophic maxillary anterior area: a case report. *Implant Dentistry* **16**: 227-234.

Lehmann, W., Edgar, C. M., Wang, K., Cho, T. J., Barnes, G. L., Kakar, S., Graves, D. T., Rueger, J. M., Gerstenfeld, L. C., & Einhorn, T. A. (2005) Tumor necrosis factor alpha (TNF-alpha) coordinately regulates the expression of specific matrix metalloproteinases (MMPS) and angiogenic factors during fracture healing. *Bone* **36**: 300-310.

Lieberman, J. R., & Friendlaender, G. E. (2005) Bone regeneration and repair: biology and clinical applications. Totowa, N.J.: Humana Press.

Livak, K. J., & Schmittgen, T. D. (2001) Analysis of relative gene expression data using real-time quantitative PCR and the 2(-delta delta C(T)) method. *Methods* **25**: 402-408.

Lobene, R. R., & Glickman, I. (1963) The response of alveolar bone to grinding with rotary diamond stones. *Journal of Periodontology* **1**: 105-119.

Preti, G., Martinasso, G., Peirone, B., Navone, R., Manzella, C., Muzio, G., Russo, C., Canuto, R. A., & Schierano, G. (2007) Cytokines and growth factors involved in the osseointegration of oral titanium implants positioned using piezoelectric bone surgery versus a drill technique: a pilot study in minipigs. *Journal of Periodontology* **78**: 716-722.

Rundle, C. H., Wang, H., Yu, H., Chadwick, R. B., Davis, E. I., Wergedal, J. E., Lau, K. H., Mohan, S., Ryaby, J. T., & Baylink, D. J. (2006) Microarray analysis of gene expression during the inflammation and endochondral bone formation stages of rat femur fracture repair. *Bone* **38**: 521-529.

Sohn, D. S., Ahn, M. R., Lee, W. H., Yeo, D. S., & Lim, S. Y. (2007) Piezoelectric osteotomy for intraoral harvesting of bone blocks. *The International Journal of Periodontics & Restorative Dentistry* **27**: 127-131.

Sohn, D. S., Lee, J. S., An, K. M., & Choi, B. J. (2009) Piezoelectric internal sinus elevation (PISE) technique: a new method for internal sinus elevation. *Implant Dentistry* **18**: 458-463.

Stubinger, S., Robertson, A., Zimmerer, K. S., Leiggener, C., Sader, R., & Kunz, C. (2006) Piezoelectric harvesting of an autogenous bone graft from the zygomaticomaxillary region: case report. *The International Journal of Periodontics and Restorative Dentistry* **26**: 453-457.

Vercellotti, T., De Paoli, S., & Nevins, M. (2001) The piezoelectric bony window osteotomy and sinus membrane elevation: introduction of a new technique for simplification of the sinus augmentation procedure. *The International Journal of Periodontics and Restorative Dentistry* **21**: 561-567.

Vercellotti, T., & Pollack, A. S. (2006) A new bone surgery device: sinus grafting and periodontal surgery. *Compendium of Continuing Education in Dentistry* **27**: 319-325.

Wallace, S. S., Mazor, Z., Froum, S. J., Cho, S. C., & Tarnow, D. P. (2007) Schneiderian membrane perforation rate during sinus elevation using piezosurgery: clinical results of 100 consecutive cases. *The International Journal of Periodontics and Restorative Dentistry* **27**: 413-419.

Wood, D. L., Hoag, P. M., Donnenfeld, O. W., & Rosenfeld, L. D. (1972) Alveolar crest reduction following full and partial thickness flaps. *Journal of Periodontology* **43**: 141-144.

PART II:

μCT AND HISTOLOGICAL COMPARISON OF WOUND HEALING RESPONSE FOLLOWING *IN VIVO* BONE INSTRUMENTATION WITH PIEZOTOME® ULTRASONIC SURGICAL UNITS AND HIGH SPEED ROTARY INSTRUMENTATION

Abstract

This study compared the radiographic and histological wound healing responses of bone to piezoelectric or high speed rotary instrumentation. Eight Sprague-Dawley rats underwent bilateral tibial osteotomies (n=16) prepared in a randomized split-leg design using high speed rotary (R) (n=7), 1st Generation Piezotome® (P1) (n=5), or 2nd Generation Piezotome® (P2) (n=4) instrumentation. At 3 weeks, qualitative histologic evaluation and quantitative μCT analysis assessed percentage bone fill (%BF) and bone mineral density (BMD) in the defect, peripheral, and distant regions. No differences in %BF or BMD were detected between groups within the osteotomy defect. Significant differences in %BF ($p=0.020$) and BMD ($p=0.008$) were noted along the peripheral region between P2 and R groups. No significant decreases in BMD were noted in peripheral sites compared to distant sites following piezoelectric instrumentation. Histologically, smooth osteotomy margins were present following piezoelectric instrumentation. These findings indicate that piezoelectric instrumentation favors preservation of bone adjacent to osteotomies.

INTRODUCTION

The piezoelectric effect, where solid crystalline materials (including quartz, silica, and ceramic) (O'Brien, 2007; Poblete-Michel & Michel, 2009) become electrically polarized under mechanical stress, was first reported by Jacques and Pierre Curie in 1880. The converse of this, the principle that the application of electricity to a crystalline material is capable of producing crystal expansion and consequent mechanical movement – the indirect piezoelectric effect – was later described by Gabriel Lippmann in 1881 (Katzir, 2006; O'Brien, 2007). This indirect piezoelectric effect is the principal by which piezoelectric systems function in dental applications.

Dental piezoelectric surgical units function by the application of electrical current to polarized quartz or ceramic disks oriented in the long-axis of a surgical handpiece. When current is applied in an alternating fashion, the ceramic elements undergo rhythmic lengthening and shortening movements. This generated mechanical energy is transmitted to a surgical tip attached to the handpiece, resulting in the linear movement and vibration of the tip. This movement is capable of cutting through mineralized tissues. An amplifier acts to increase the amount of movement and vibration within the surgical tip (Poblete-Michel & Michel, 2009), permitting tip vibrations commonly in the range of 60-200 μm (Schlee et al., 2006), a degree of movement that optimizes the cutting potential.

There are four primary advantages of piezosurgical units, including selective cutting action, increased precision, improved visibility, and greater surgical accessibility (Poblete-Michel & Michel, 2009). First, piezoelectric surgical units oscillate at an ultrasonic frequency of 25 – 30 kHz, a frequency at which mineralized tissues – such as bone – are selectively cut while nerves, blood vessels, and other soft tissues are not injured. A frequency greater than 50 kHz is required to cut these soft tissues (Schlee et al., 2006). This characteristic is especially useful in a variety of surgical procedures that pose an increased risk of damage to soft tissues, such as lateral window sinus lifts or surgical procedures adjacent to nerves. Second, piezosurgical units offer increased precision in that no macromovements are generated during the use of the vibrating surgical tip, permitting the generation of narrower and more precise cuts (Poblete-Michel & Michel, 2009). Third, increased visibility is a consequence of the cavitational effect by which irrigational water bubbles implode, mechanically removing debris and blood (Poblete-Michel & Michel, 2009). Finally, improved surgical accessibility is present due to the design of the different surgical tips.

Currently, there are greater than 50 articles detailing the use and advantages of piezoelectric surgical units in a variety of surgical treatments, including lateral window sinus lift techniques (Sohn et al., 2009; Vercellotti et al., 2001; Wallace et al., 2007), autogenous bone grafting (Happe, 2007; Sohn et al., 2007; Stubinger et al., 2006), implant site preparation (Preti et al., 2007), osteotomy close to nerves (Bovi et al., 2010; Geha et al., 2006), extractions (Degerliyurt et al., 2009; Grenga & Bovi, 2004), periodontal surgery (Vercellotti & Pollack, 2006), and distraction osteogenesis (Gonzalez-Garcia et al., 2008; Lee et al., 2007). Despite its common use in clinical practice, there is limited literature

published detailing the biologic wound healing response to piezoelectric surgery or any biological advantages of this surgical modality.

The purpose of this present study is to compare the effects of the first- and second-generation Piezotome® (Satelec Acteon Group, Merignac, France) surgical units on osseous healing to traditional high speed rotary instrumentation using radiographic and histologic approaches in a rat tibia model. Our hypothesis is that the histologic and radiographic appearance, and general tissue regeneration responses of bone to instrumentation using first- and second-generation Piezotome units is equivalent or better than rotary instrumentation.

MATERIALS AND METHODS

Surgical Procedures

All experimental procedures followed a protocol approved by the Institutional Animal Care and Use Committee at The University of North Carolina at Chapel Hill. Eight male Sprague-Dawley rats (Charles River Laboratories International, Inc., Wilmington, MA) weighing approximately 250-300g were used for the study for a total of 16 tibiae. Rats were anesthetized with an intraperitoneal injection of ketamine/xylazine and the surgical sites shaved and disinfected with Betadine®. An incision was made along the medial aspect of each tibia. The overlying muscle was gently separated and the periosteum elevated. Using a randomized approach, a 6mm vertical osteotomy was prepared through the cortical bone in the medial aspect of each tibia using copious saline irrigation and either (1) the BS1 insert (Satelec Acteon, Merignac, France) mounted on the Piezotome® (Acteon) surgical unit (n = 4 tibiae) (P1 group), (2) the BS1 insert mounted on the Implant Center 2 (Piezotome® 2, Acteon) surgical unit (n = 5 tibia) (P2 group), or (3) a ¼ round bur (Brassler USA, Savannah, GA) with high speed rotary instrumentation (n = 7 tibiae, Implant Center 2, Acteon) (R group). The power and irrigation settings were as follows: P1: Mode 1, 50 mL/min irrigation; P2: Mode D1, 60 mL/min irrigation; and R: 200,000 revolutions per

minute, 60 mL/min irrigation. Following surgery, the periosteal/muscle tissues were sutured using 5-0 chromic gut followed by closing of flaps with 4-0 silk suture.

After 3 weeks of healing, the rats were euthanized by CO_2 inhalation and cardiac perfusion fixation completed using 10% formalin. Tibiae were isolated at the level of articulation, fixed in 10% neutral buffered formalin (NBF) for 48 hours, rinsed in phosphate buffered saline (PBS), and stored in 70% ethanol at 4°C.

μCT Analysis

Following fixation, tibiae were scanned using the Skyscan 1074HR microCT (Skyscan, Aartselaar, Belgium) and the Skyscan acquisition and the NRecon reconstruction software at a resolution of 20.5 μm/pixel. Standardized scanning (40 kV source voltage, 1000 μA source current, 540 ms exposure, 206 projections per 180° rotation) and reconstruction settings were used to produce cross-sectional images. All images had a pixel size of 20.7μm x 20.7μm with 20.7μm distance between consecutive cross-sectional images. For calibration to determine bone mineral densities within regions of interest (ROIs), hydroxyapatite phantoms (Computerized Imaging Reference Systems, Inc., Norfolk, VA) of 500 mg/cc and 1000mg/cc densities were utilized under identical scanning and reconstruction parameters. CTAn software (Skyscan) was used to analyze the microCT scans.

The defect midpoint was identified in the long axis of each tibia and analyses were completed to include the defect 2mm proximal to the midpoint and 2mm distal to the midpoint, for a total defect length of 4mm (194 of 511 cross-sectional images). Three separate ROIs were selected for analysis representing the central defect and two peripheral

regions (Figure 1). Each ROI was selected at 200% within the axial cross-section images approximating the margins of the cortical bone and analysis was completed on any material contained within the ROI. For the ROI corresponding to the central defect, the width of the ROI was measured to correspond to the width of the instrument used to create the cortical osteotomy (0.50mm for the ¼ round bur used in rotary instrumentation and 0.60mm for the BS1 insert used in Piezotome 1 and Piezotome 2 instrumentation). Two peripheral ROIs with a width of 0.25mm immediately adjacent to the defect ROI were evaluated to assess the effects of the different instrumentation methods on peripheral bone. A distant ROI with a width of 0.25mm on a surface without periosteal soft tissue elevation or osteotomy preparation was also evaluated to compare the effects of different instrumentation methods on distant bone. Bone volume fraction (BV/TV) and the average volumetric mineral density of the mineralized tissue (BMD in mg/cc) were quantified. For each sample, the values for the two peripheral regions were averaged prior to statistical analyses.

Histology

Tissues fixed in 10% NBF were rinsed in PBS and demineralized by immersion in Immunocal (Decal Chemical Corporation, Tallman, NY) for 2 weeks at room temperature. Complete decalcification was confirmed by lack of radiopacity using additional microCT scans. Tissues were processed with routine ethanol dehydrations, xylene clearing, and paraffin infiltrations. Specimens were axially sectioned at a thickness of 5 μm, deparaffinized, and stained with hematoxylin and eosin for gross light microscopic analysis. Samples were qualitatively assessed.

Statistics

Statistical analyses of microCT data was performed using SPSS 17.0 software (SPSS, Inc., Chicago, IL). The one-way ANOVA statistical test was used to evaluate differences in the percentage of bone fill and bone mineral density in the defect and peripheral ROIs. Tukey post-hoc analysis was used to identify statistically significant differences (p-values $\leq$ 0.05) between the groups. Data is presented as mean ± standard deviation.

RESULTS

Safety

All rats healed unremarkably with no detectable differences in healing or notable post-operative discomfort identified between the groups throughout the duration of the three week healing period. Histologically, there was no evidence of any exuberant inflammatory events, with no notable differences in the inflammatory response between groups. Similarly, there was no evidence of any pathological features radiographically.

Percentage of Bone Fill (%) in Osteotomy Defect, Immediately Adjacent Periphery, and Distant Regions

In the central osteotomy defect regions, there were no statistically significant differences ($p = 0.830$) in the percentage of bone fill (%BF) following instrumentation with P1 ($31.63 \pm 15.94\%$), P2 ($36.87 \pm 15.64\%$), and R ($32.73 \pm 11.56\%$). However, compared to R ($59.43 \pm 12.89\%$), there was a statistically significant increase in the percentage of bone fill in the peripheral region immediately adjacent to the central osteotomy following instrumentation with P2 ($79.70 \pm 10.32\%$; $p = 0.020$), but not with P1 ($72.13 \pm 7.50\%$; $p =$

0.198). There was no statistically significant difference in percentage of bone fill between P1 and P2 treatment groups ($p = 0.577$) (Table 1 & Figure 2).

Relative to distant regions, there were statistically significant differences in the percentage of bone fill in the central osteotomy defect and immediately peripheral regions for all three treatment groups (Table 2 & Figure 2).

Bone Mineral Density (mg/cc) in Osteotomy Defect, Immediately Adjacent Periphery, and Distant Regions

In the central osteotomy defect regions, there were no statistically significant differences in bone mineral density between the three treatment groups (P1: 0.51 ± 0.17 mg/cc; P2: 0.60 ± 0.13 mg/cc; R: 0.55 ± 0.10 mg/cc; $p = 0.607$). However, similar to percent bone fill, there was a statistically significant increase in the bone mineral density in the peripheral region immediately adjacent to the central osteotomy following instrumentation with P2 (0.98 ± 0.08 mg/cc; $p = 0.008$) compared to R (0.79 ± 0.10 mg/cc), but not with the P1 (0.90 ± 0.08 mg/cc; $p=0.160$). Similarly, there was no statistically significant difference in bone mineral density between P1 and P2 treatment groups ($p = 0.403$) (Table 1 & Figure 3).

Relative to distant regions, there were statistically significant differences in the bone mineral density of the central osteotomy defect for all three treatment groups. However, there was a statistically significant decrease in the bone mineral density only between the immediately adjacent periphery and distant regions following rotary instrumentation ($p < 0.0001$).

Equivalence Testing

For each region of interest, equivalence testing was completed using 95% confidence intervals compared to a zone of clinical indifference determined by the standard deviation following rotary instrumentation (Appendix A). Equivalence testing supports the statistical analyses, indicating that the three treatment groups are equivalent in regards to percentage of bone fill and bone mineral density in the central osteotomy and distant sites. Non-equivalence, however, is suggested between rotary R and P2 in regards to bone mineral density in sites peripheral to the osteotomy.

Descriptive Histology of Bone Healing

Histologically, the healing of the osteotomies was very similar between the P1 and P2 groups at 3 weeks. Bone healing correlated with radiographic findings (Figure 4). Furthermore, there were minimal differences apparent in the quality of the regenerated bone within the osteotomy defects following the three different treatment modalities. In a number of sections in which rotary instrumentation was performed (Figure 5), the remodeling process appeared to extend laterally relative to the osteotomy site, a feature not characteristic of the osteotomy sites prepared by piezoelectric instrumentation. Following P1 (Figure 6) or P2 (Figure 7) instrumentation, the osteotomy margins were smooth and much better defined in a majority of the samples at 3 weeks, suggesting minimal post-operative necrosis of the marginal bone during the healing process following piezoelectric instrumentation. This feature was inconsistently identified in the samples following rotary instrumentation. In all

samples, osteoblasts lined the inner aspect of the bone, including the newly formed bone within the defect. Incremental lines were present, indicating bone apposition, and minimal inflammatory cells were also present at 3 weeks.

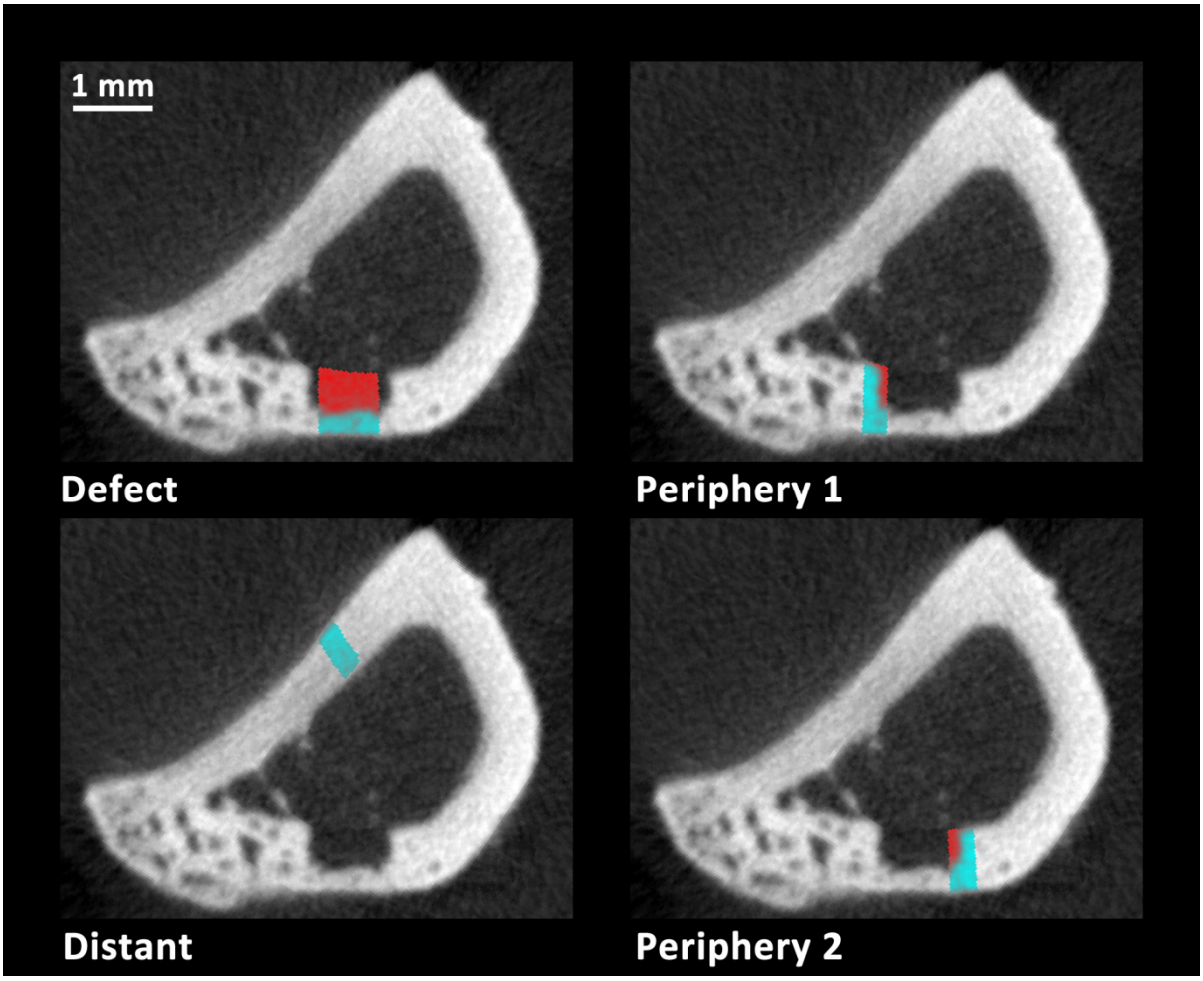

Figure 1. ROI Selections for μCT Analysis. μCT cross-section of the tibiae 3 weeks after ultrasonic osteotomy preparation demonstrating measured ROI selections for μCT analysis with the CTAn software. The width of the Defect ROI was 0.50mm for R instrumentation and 0.60mm for both P1 and P2 instrumentation. The width of the Periphery 1, Periphery 2, and Distant ROIs was 0.25mm. Each peripheral ROI (left and right) was analyzed separately with the mean value of each sample used for analysis.

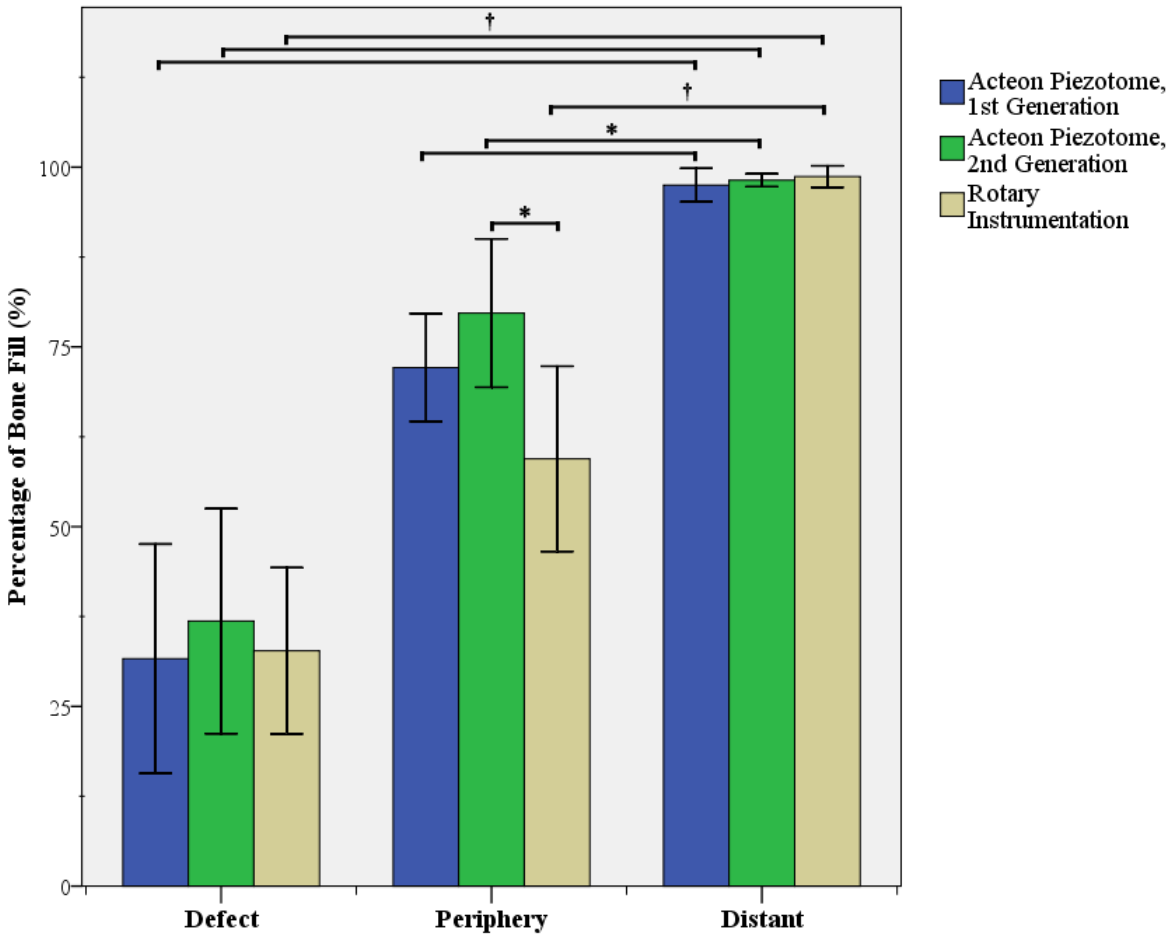

Figure 2. Percentage of Bone Fill at 3 Weeks. μCT analysis of the bone fill (mean (%) ± standard deviation) at 3 weeks post-surgery in the central defect, periphery, and distant region of interests (ROIs) following osteotomy with P1, P2, and R instrumentation. *Significant difference between treatment groups at $p < 0.05$. †Significant difference between treatment groups at $p < 0.01$.

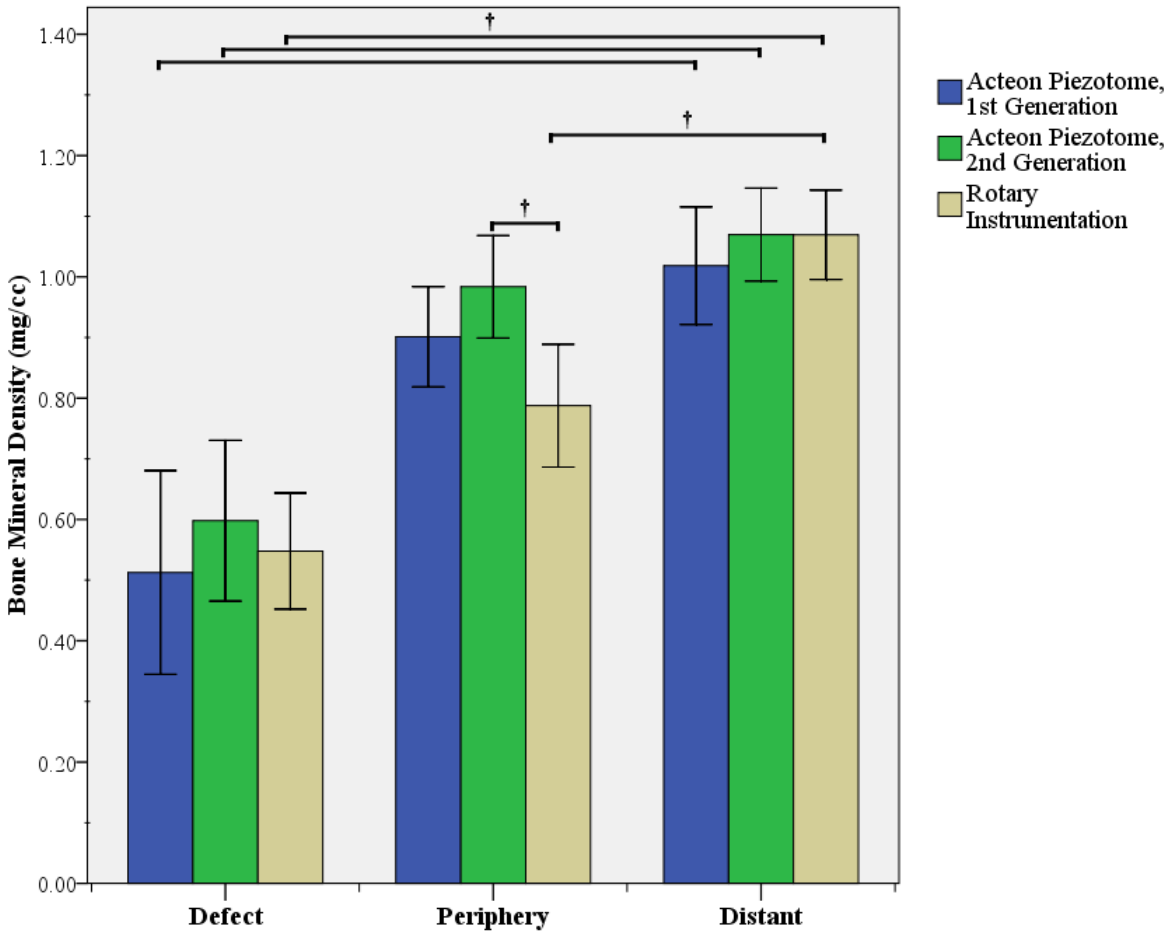

Figure 3. Bone Mineral Density (mg/cc) at 3 Weeks. μCT analysis of bone mineral density (mean (mg/cc) ± standard error) at 3 weeks post-surgery in the central defect and periphery region of interests (ROIs) following osteotomy with P1, P2, and R instrumentation. *Significant difference between treatment groups at $p < 0.05$. †Significant difference between treatment groups at $p < 0.01$.

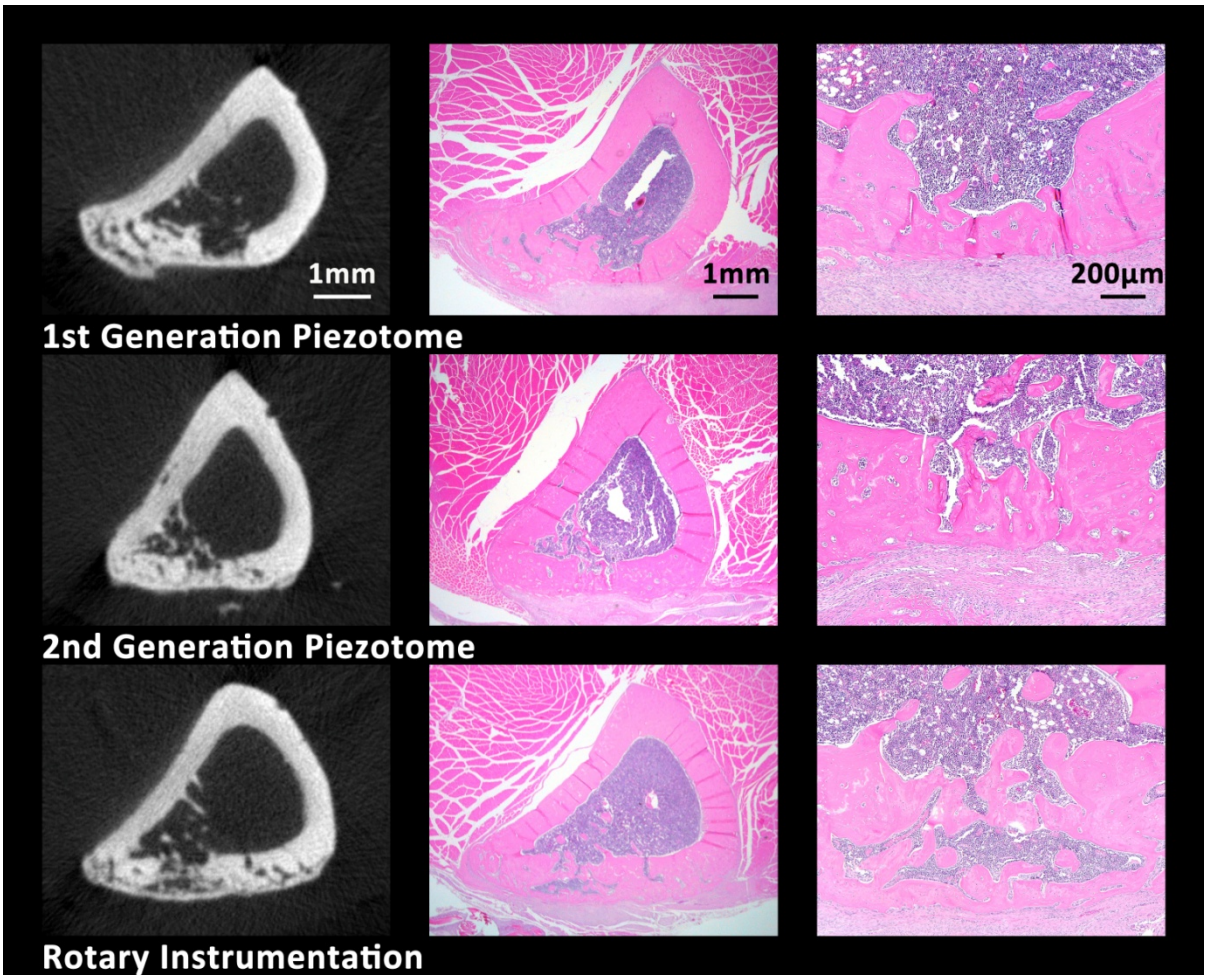

Figure 4. Radiographic and Histologic Signs of Healing at 3 Weeks Post-Surgery. Bone healing identified histologically within the osteotomy defect correlated with radiographic findings at 3 weeks.

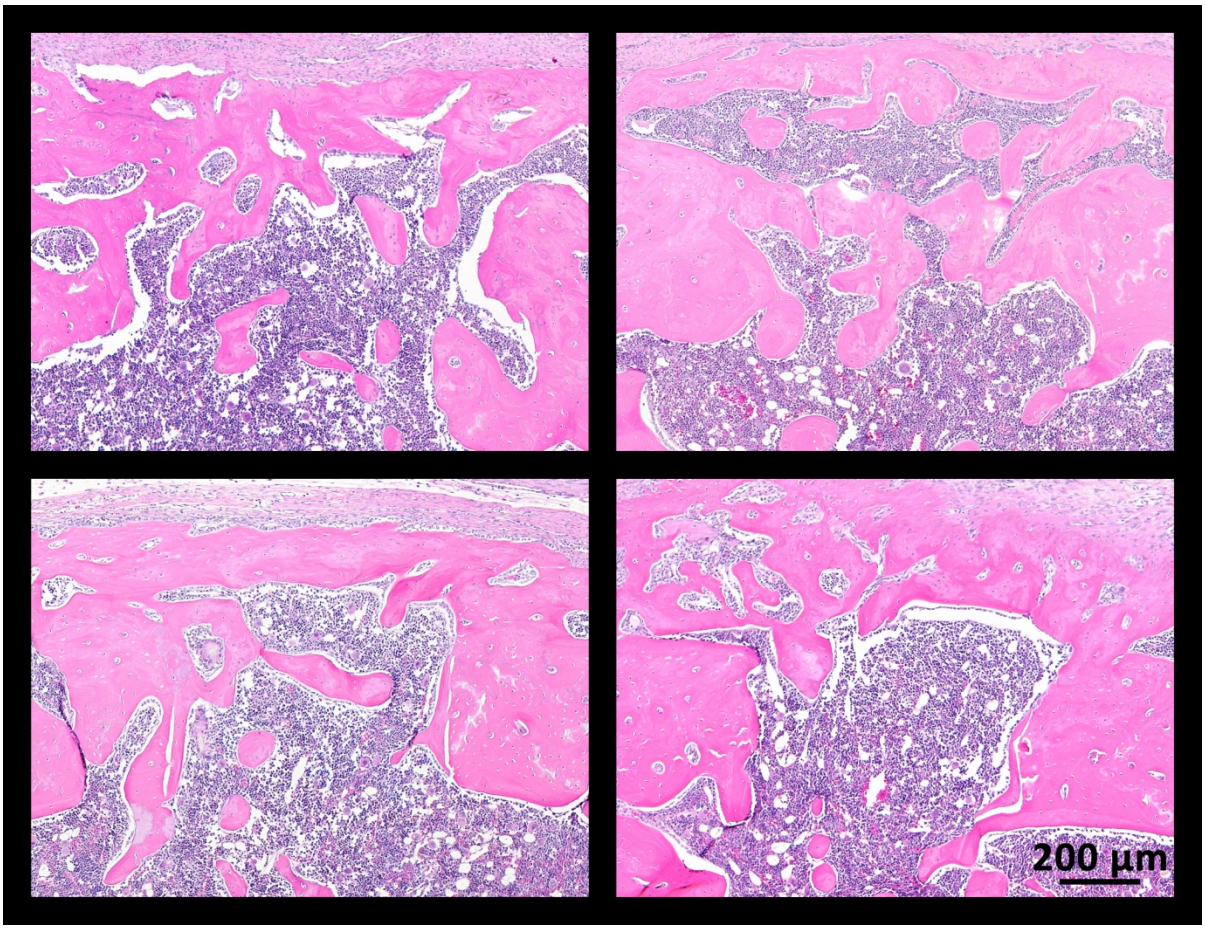

Figure 5. Histology following High Speed Rotary Instrumentation. Following instrumentation with R, osteotomy surfaces are largely irregular with some samples exhibiting smooth surfaces. Furthermore, peripheral regions appear to have greater resorption and osseous irregularities relative to samples with P1 or P2 instrumentation.

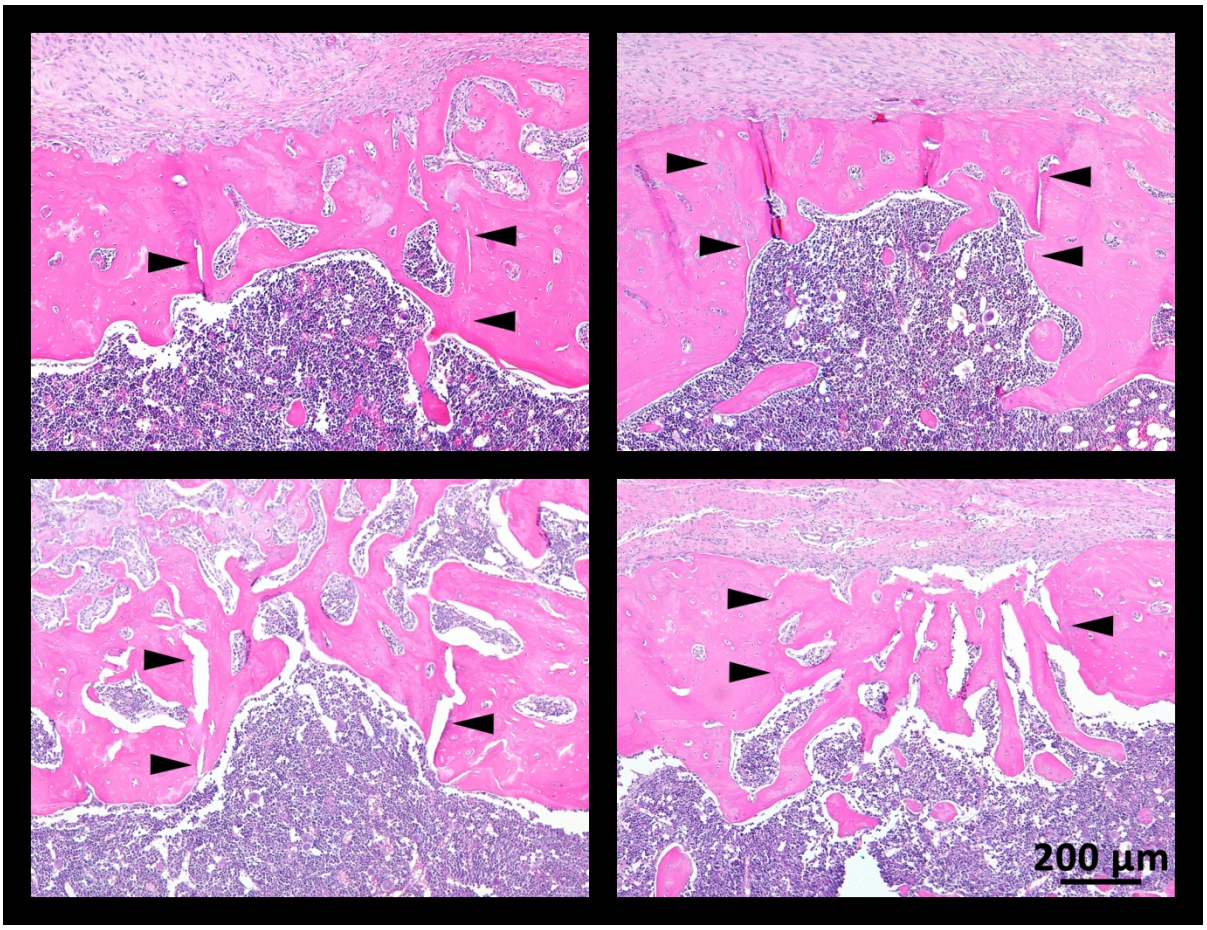

Figure 6. Histology following 1st Generation Piezotome® Instrumentation. Following instrumentation with P1, smooth osteotomy surfaces are present with newly formed bone either adjacent to or in immediate contact with the osteotomy surface. Arrowheads are used to denote the smooth osteotomy margins.

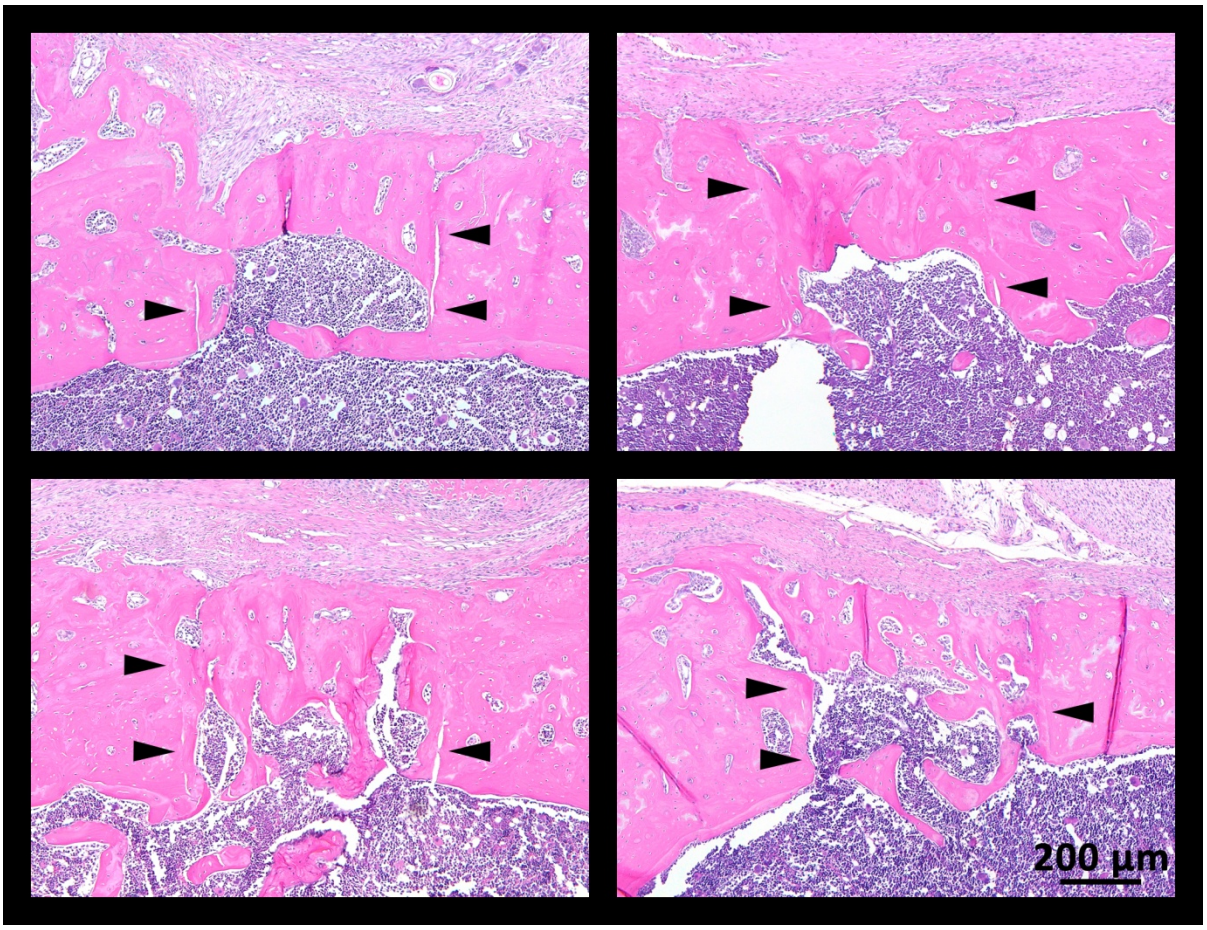

Figure 7. Histology following 2nd Generation Piezotome® Instrumentation. Following instrumentation with P2, smooth osteotomy surfaces are present with newly formed bone either adjacent to or in immediate contact with the osteotomy surface. Arrowheads are used to denote the smooth osteotomy margins.

Table 1. ***Percentage of Bone Fill and Bone Mineral Density (mg/cc) at 3 week within Different ROI Locations*****. µCT data (mean ± standard deviation) for bone fill (%) and bone mineral density (mg/cc) in the central osteotomy defects, immediately adjacent peripheral bone, and distant regions at 3 weeks post-surgery.**

	DEFECT		PERIPHERY		DISTANT	
	Bone Fill (%)	Bone Mineral Density (mg/cc)	Bone Fill (%)	Bone Mineral Density (mg/cc)	Bone Fill (%)	Bone Mineral Density (mg/cc)
1st Generation Piezotome® (P1) (n=4)	31.63 ± 15.94	0.51 ± 0.17	72.13 ± 7.50	0.90 ± 0.08	97.51 ± 2.32	1.02 ± 0.10
2nd Generation Piezotome® (P2) (n = 5)	36.87 ± 15.64	0.60 ± 0.13	79.70 ± 10.32*	0.98 ± 0.08†	98.18 ± 0.90	1.07 ± 0.08
Rotary Instrumentation (R) (n = 7)	32.73 ± 11.56	0.55 ± 0.10	59.43 ± 12.89	0.79 ± 0.10	98.68 ± 1.50	1.07 ± 0.07

* $p < 0.05$ within location compared to R. † $p < 0.01$ within location compared to R.

Table 2. Percentage of Bone Fill and Bone Mineral Density (mg/cc) at 3 week within Treatment Groups**. µCT data (mean ± standard deviation) for bone fill (%) and bone mineral density (mg/cc) in the central osteotomy defects, immediately adjacent peripheral bone, and distant regions at 3 weeks post-surgery.**

	DEFECT		PERIPHERY		DISTANT	
	Bone Fill (%)	Bone Mineral Density (mg/cc)	Bone Fill (%)	Bone Mineral Density (mg/cc)	Bone Fill (%)	Bone Mineral Density (mg/cc)
1st Generation Piezotome® (P1) (n=4)	31.63 ± 15.94†	0.51 ± 0.17†	72.13 ± 7.50*	0.90 ± 0.08	97.51 ± 2.32	1.02 ± 0.10
2nd Generation Piezotome® (P2) (n = 5)	36.87 ± 15.64†	0.60 ± 0.13†	79.70 ± 10.32*	0.98 ± 0.08	98.18 ± 0.90	1.07 ± 0.08
Rotary Instrumentation (R) (n = 7)	32.73 ± 11.56†	0.55 ± 0.10†	59.43 ± 12.89†	0.79 ± 0.10†	98.68 ± 1.50	1.07 ± 0.07

* $p < 0.05$ within treatment group compared to distant location. † $p < 0.01$ within treatment group compared to distant location. †

DISCUSSION

While the clinical effectiveness of piezoelectric surgery continuous to be well documented, the tissue response to this form of surgical instrumentation is not completely understood. We compared the osseous healing responses to osteotomies prepared using piezoelectric and conventional rotary instrumentation using radiographic and histological techniques and also compared two piezoelectric surgical units with different power output capacities. The rationale for the latter comparison is to assess the potential for tissue damage at the higher power output.

There were no detectable differences in healing and animal behavior after instrumentation with any of the three different treatment modalities throughout the duration of the healing period. When we evaluated percent bone fill and bone mineral density at the central and peripheral aspects of the osteotomies, there was a significant increase in the percentage of bone fill and bone mineral density in the peripheral region immediately adjacent to the osteotomy, but not in the central aspect of the osteotomy following instrumentation with P2 relative to R. When compared to bone at distant regions, there were no statistical differences in bone mineral density between the central region of the osteotomy site between groups. However, there were statistically significant differences in bone mineral density along the periphery of the osteotomy compared to the R group, indicating

less mineralization of bone at sites instrumented with R relative to P1 or P2. Histologically, the margins of the osteotomy surfaces were exceptionally smooth following piezoelectric instrumentation.

Concerns that the added power in the P2 unit may be detrimental to osseous tissues, potentially impeding the osseous healing process, are not supported by this study. Previous studies have described factors that may influence osseous healing include temperature, post-instrumentation microstructure, and blood perfusion (von See et al., 2011). Bone necrosis occurs during osteotomy preparation when the bone temperature exceeds 47°C for 1 minute (Albrektsson & Eriksson, 1985). Harder et al. (2009), reported first generation Piezotome® units produced a median temperature increase of 1.2°C, while other ultrasonic piezoelectric units examined produced median temperature increases of 2.5-3.1°C on bone specimens at room temperature (21°C), well below the 47°C threshold. In these laboratory conditions, the bone temperature increases during piezoelectric instrumentation are below that necessary to cause necrosis. While a benefit of piezoelectric surgery is improved visibility of the surgical site due to the cavitation effect, we did not find histologic evidence of intraosseous vascular thrombosis or occlusion of adjacent bone that might occur following piezoelectric instrumentation, which is supported by other studies (von See et al., 2011). Consequently, blood supply to the remaining osseous tissue appears to be preserved. There is no known evidence at this time to support the theory that the added power found in the P2 unit will either impair the healing process or more directly damage peripheral bone. Although we did not evaluate these specific factors, the lack of tissue necrosis and the presence of a minimal inflammatory infiltrate in samples instrumented at the higher power output suggest that they were minimally impacted.

Evidence suggests that micro-cracks form during plastic deformation of bone and act to mechanically damage canalicular spaces and promote osteocyte apoptosis (Noble & Reeve, 2000; Rochefort, Pallu, & Benhamou, 2010). Damage to canalicular spaces during osteotomy preparation may be expected to have a similar effect on osteocyte viability. Following piezoelectric ultrasonic instrumentation, bone microstructure and the vitality of osteocytes adjacent to the cut surface is preserved (Hollstein et al., 2011). In normal bone homeostasis, osteocyte cell death promotes osteoclast recruitment and subsequent resorption through complex cell signaling during the initial stages of repair (Nakahama, 2010). Maintenance of peripheral cellular vitality may act to minimize cellular signaling processes contributing to osseous resorptive processes, while the intact bony margins may provide a solid surface for osteoblasts adherence and osteoid deposition. Indeed, bone apposition was readily apparent on peripheral surfaces forming an osseous bridge spanning the outer aspect of the osteotomy defect. While the defect margins were still identifiable histologically, the newly regenerated bone was largely in direct contact with the previously cut bone and in some locations indistinguishable from the preexisting bone. While radiographic differences were noted in the quality of the bone within peripheral sites following R instrumentation relative to either P1 or P2, there were no histologically notable differences in the quality of the bone between P1 and P2 in either the central or peripheral osteotomy sites. Anecdotally, osteotomies prepared using P2 were completed faster than with P1. When taken together, these findings suggest that the increased power and speed of the P2 unit was not detrimental to the bone immediately adjacent to the osteotomy compared to the other instrumentation methods studied.

This radiographic and histologic study points to favorable osseous wound healing when piezoelectric instrumentation is used as the surgical modality, including the P2 unit with its higher power output capacity. Additional studies with larger numbers of animals are required to confirm our findings and to further investigate the effects of piezoelectric energy on osseous wound healing factors at the tissue and cellular level, specifically osteocyte and osteoblast function.

CONCLUSIONS

There are no statistically significant differences in the amount of bone fill or bone mineral density radiographically in the central osteotomy defects following P1, P2, and R instrumentation at 3 weeks. There is increased bone fill and bone mineral density in the region immediately peripheral to the central defect following osteotomy preparation with P2 compared to R. Furthermore, there are no significant differences in the bone mineral density between the bone immediately peripheral to the central osteotomy defects and distant sites following instrumentation with either P1 or P2. Histologically, bone fill within osteotomy sites prepared with P1 or P2 instrumentation appear to have increased osseous organization and maturity relative to R instrumentation. Additionally, no adverse effects were identified either radiographically or histologically following instrumentation with P1 or P2 units. Future studies should be aimed at confirming these findings with larger treatment groups and evaluating the effects of the different treatment modalities on intramembranous bone healing.

REFERENCES

Albrektsson, T., & Eriksson, A. (1985) Thermally induced bone necrosis in rabbits: Relation to implant failure in humans. *Clinical Orthopaedics and Related Research* **195**: 311-312.

Bovi, M., Manni, A., Mavriqi, L., Bianco, G., & Celletti, R. (2010) The use of piezosurgery to mobilize the mandibular alveolar nerve followed immediately by implant insertion: a case series evaluating neurosensory disturbance. *The International Journal of Periodontics and Restorative Dentistry* **30**: 73-81.

Degerliyurt, K., Akar, V., Denizci, S., & Yucel, E. (2009) Bone lid technique with piezosurgery to preserve inferior alveolar nerve. *Oral Surgery, Oral Medicine, Oral Pathology, Oral Radiology, and Endodontics* **108**: e1-5.

Geha, H. J., Gleizal, A. M., Nimeskern, N. J., & Beziat, J. L. (2006) Sensitivity of the inferior lip and chin following mandibular bilateral sagittal split osteotomy using piezosurgery. *Plastic and Reconstructive Surgery* **118**: 1598-1607.

Gonzalez-Garcia, A., Diniz-Freitas, M., Somoza-Martin, M., & Garcia-Garcia, A. (2008) Piezoelectric and conventional osteotomy in alveolar distraction osteogenesis in a series of 17 patients. *The International Journal of Oral and Maxillofacial Implants* **23**: 891-896.

Grenga, V., & Bovi, M. (2004) Piezoelectric surgery for exposure of palatally impacted canines. *Journal of Clinical Orthodontics* **38**: 446-448.

Happe, A. (2007) Use of a piezoelectric surgical device to harvest bone grafts from the mandibular ramus: report of 40 cases. *The International Journal of Periodontics and Restorative Dentistry* **27**: 241-249.

Harder, S., Wolfart, S., Mehl, C., & Kern, M. (2009) Performance of ultrasonic devices for bone surgery and associated intraosseous temperature development. *The International Journal of Oral and Maxillofacial Implants* **24**: 484-490.

Hollstein, S., Hoffmann, E., Vogel, J., Heyroth, F., Prochnow, N., & Maurer, P. (2011) Micromorphometrical analyses of five different ultrasonic osteotomy devices at the rabbit skull. *Clinical Oral Implants Research* Doi: 10.1111/j.1600-0501.2011.02185.x.

Katzir, S. (2006) The beginnings of piezoelectricity: a study in mundane physics. Dordrecht: Springer.

Lee, H. J., Ahn, M. R., & Sohn, D. S. (2007) Piezoelectric distraction osteogenesis in the atrophic maxillary anterior area: a case report. *Implant dentistry* **16**: 227-234.

Nakahama, K. (2010) Cellular communications in bone homeostasis and repair. *Cellular and Molecular Life Sciences* **67**: 4001-4009.

Noble, B. S., & Reeve, J. (2000) Osteocyte function, osteocyte death and bone fracture resistance. *Molecular and Cellular Endocrinology* **159**: 7-13.

O'Brien, W. D.,Jr. (2007) Ultrasound-biophysics mechanisms. *Progress in Biophysics and Molecular Biology* **93**: 212-255.

Poblete-Michel, M. G., & Michel, J. F. (2009) Clinical success in bone surgery with ultrasonic devices. Paris, France: Quintessence International.

Preti, G., Martinasso, G., Peirone, B., Navone, R., Manzella, C., Muzio, G., Russo, C., Canuto, R. A., & Schierano, G. (2007) Cytokines and growth factors involved in the osseointegration of oral titanium implants positioned using piezoelectric bone surgery versus a drill technique: a pilot study in minipigs. *Journal of Periodontology* **78**: 716-722.

Rochefort, G. Y., Pallu, S., & Benhamou, C. L. (2010) Osteocyte: the unrecognized side of bone tissue. *Osteoporosis International* **21**: 1457-1469.

Schlee, M., Steigmann, M., Bratu, E., & Garg, A. K. (2006) Piezosurgery: basics and possibilities. *Implant dentistry* **15**: 334-340.

Sohn, D. S., Ahn, M. R., Lee, W. H., Yeo, D. S., & Lim, S. Y. (2007) Piezoelectric osteotomy for intraoral harvesting of bone blocks. *The International Journal of Periodontics & Restorative Dentistry* **27**: 127-131.

Sohn, D. S., Lee, J. S., An, K. M., & Choi, B. J. (2009) Piezoelectric internal sinus elevation (PISE) technique: a new method for internal sinus elevation. *Implant Dentistry* **18**: 458-463.

Stubinger, S., Robertson, A., Zimmerer, K. S., Leiggener, C., Sader, R., & Kunz, C. (2006) Piezoelectric harvesting of an autogenous bone graft from the zygomaticomaxillary region: case report. *The International Journal of Periodontics and Restorative Dentistry* **26**: 453-457.

Vercellotti, T., De Paoli, S., & Nevins, M. (2001) The piezoelectric bony window osteotomy and sinus membrane elevation: introduction of a new technique for simplification of the sinus augmentation procedure. *The International Journal of Periodontics and Restorative Dentistry* **21**: 561-567.

Vercellotti, T., & Pollack, A. S. (2006) A new bone surgery device: sinus grafting and periodontal surgery. *Compendium of Continuing Education in Dentistry* **27**: 319-325.

von See, C., Gellrich, N. C., Rucker, M., Kokemuller, H., Kober, H., & Stover, E. (2011) Investigation of perfusion in osseous vessels in close vicinity to piezo-electric bone cutting. *The British Journal of Oral and Maxillofacial Surgery* Doi: 10.1016/j.bjoms.2011.04.069.

Wallace, S. S., Mazor, Z., Froum, S. J., Cho, S. C., & Tarnow, D. P. (2007) Schneiderian membrane perforation rate during sinus elevation using piezosurgery: clinical results of 100 consecutive cases. *The International Journal of Periodontics and Restorative Dentistry* **27**: 413-419.

APPENDIX A:

Equivalence Testing Using Confidence Intervals

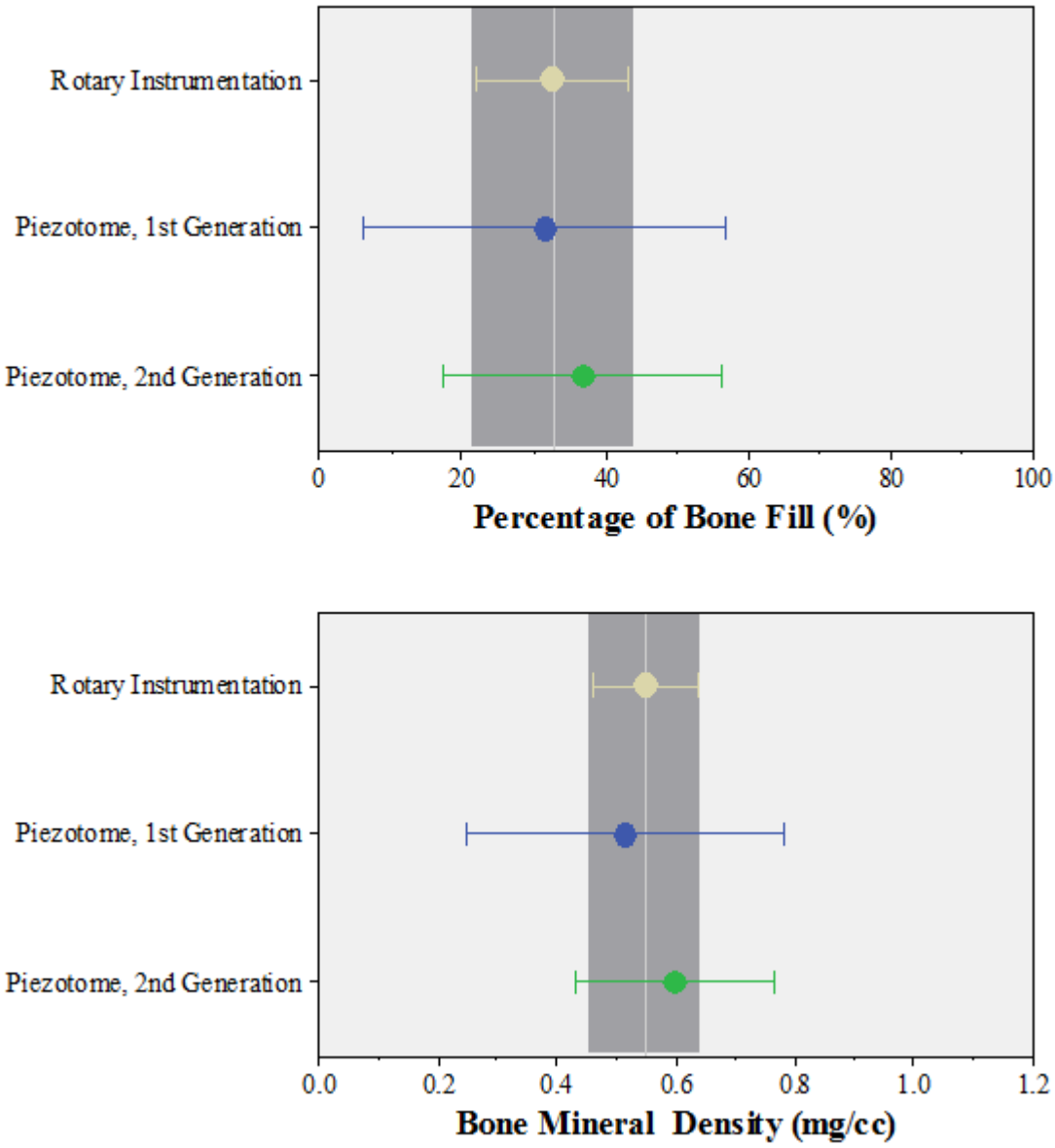

Figure 1. Equivalence Testing within the Defect ROI. Equivalence testing using 95% confidence intervals for (a) percentage of bone fill (%) and (b) bone mineral density (mg/cc) in the central defect ROI between the three treatment groups following μCT analysis. For each treatment group, mean ± 95% confidence interval is charted. The dark gray zone represents the zone of indifference as determined by the mean ± one standard deviation following rotary instrumentation.

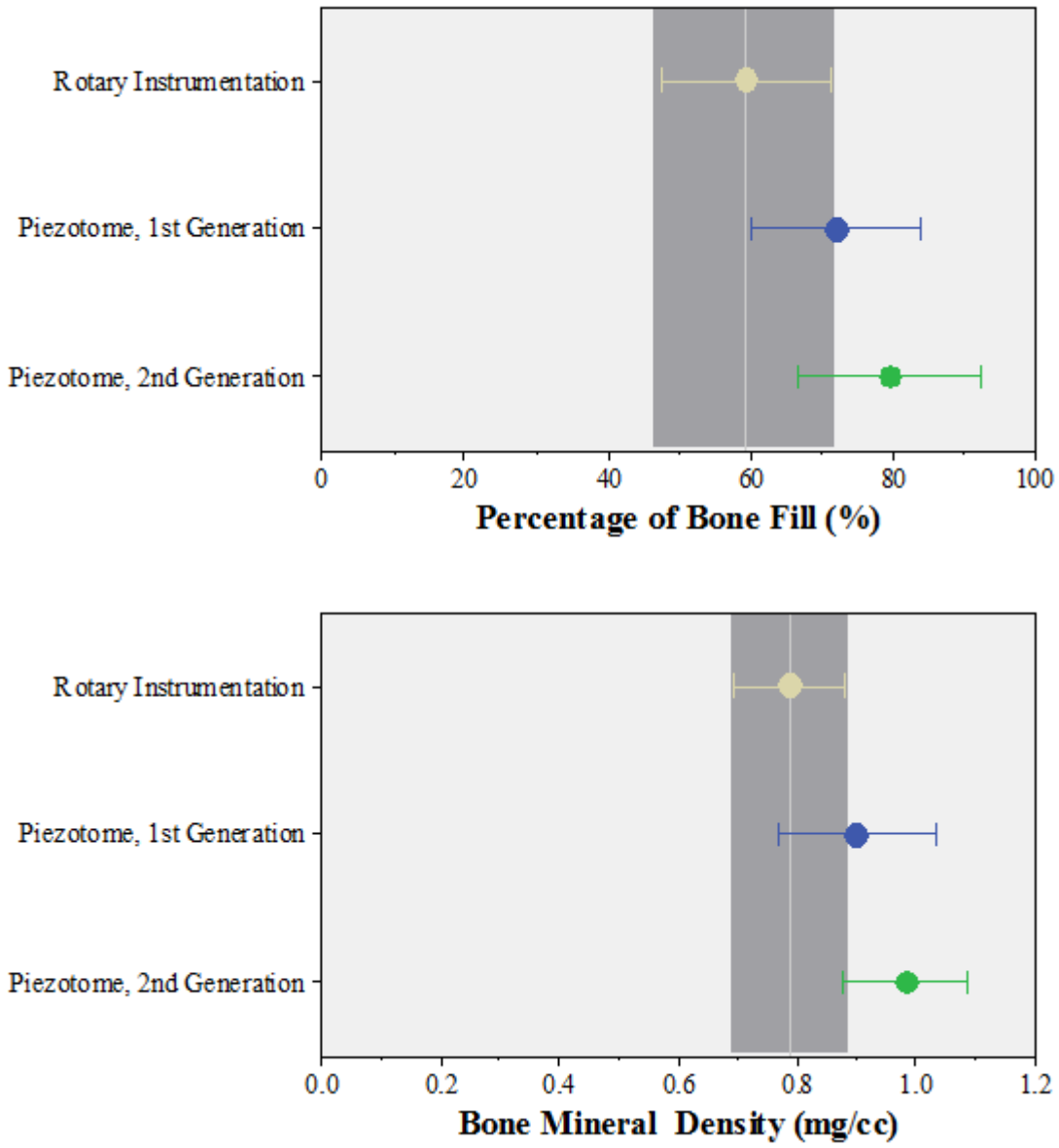

Figure 2. Equivalence Testing within the Periphery ROI. Equivalence testing using 95% confidence intervals for (a) percentage of bone fill (%) and (b) bone mineral density (mg/cc) in the periphery ROI between the three treatment groups following μCT analysis. For each treatment group, mean ± 95% confidence interval is charted. The dark gray zone represents the zone of indifference as determined by the mean ± one standard deviation following rotary instrumentation.

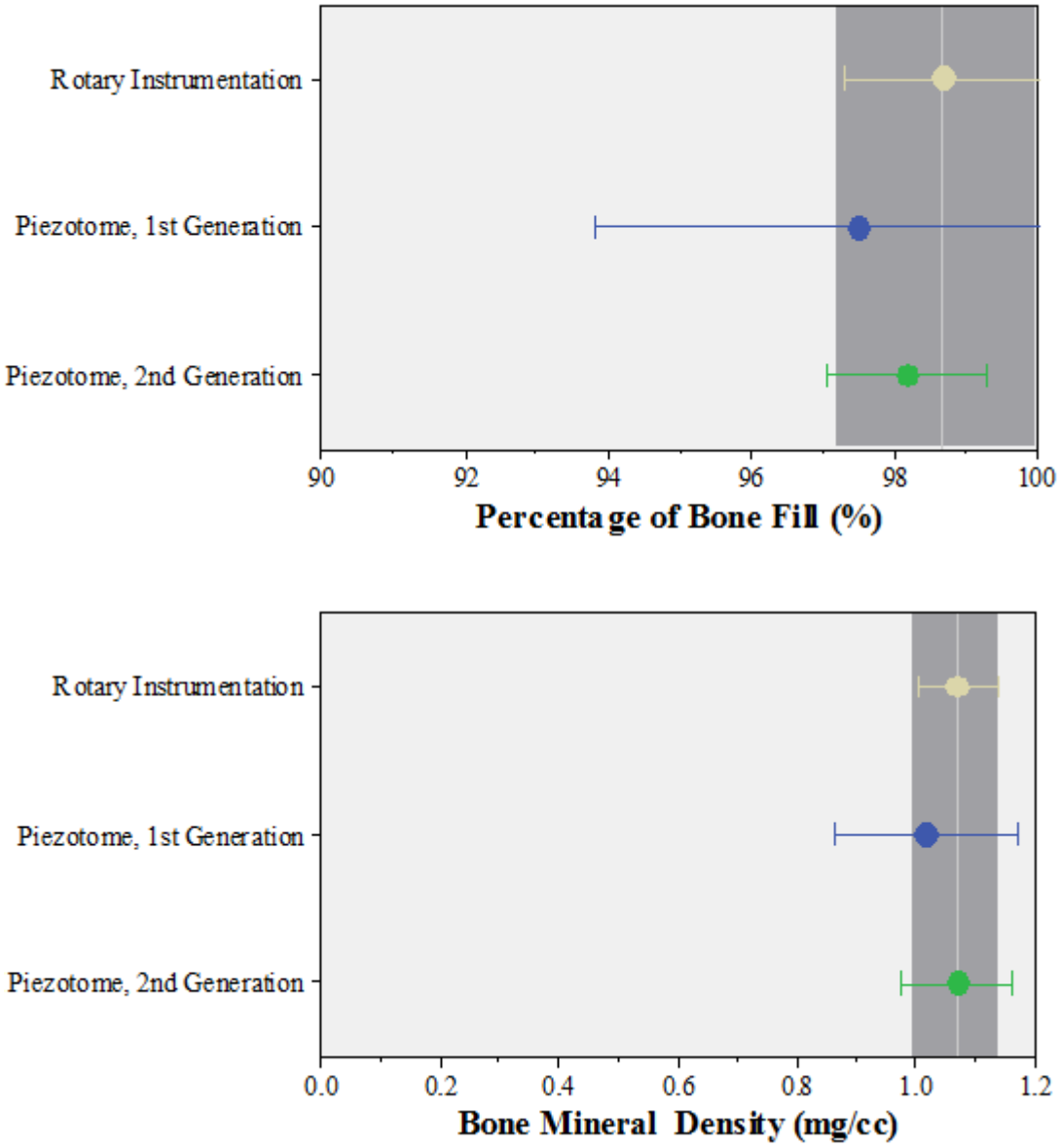

Figure 3. Equivalence Testing within the Distant ROI. Equivalence testing using 95% confidence intervals for (a) percentage of bone fill (%) and (b) bone mineral density (mg/cc) in the distant ROI between the three treatment groups following µCT analysis. For each treatment group, mean ± 95% confidence interval is charted. The dark gray zone represents the zone of indifference as determined by the mean ± one standard deviation following rotary instrumentation.

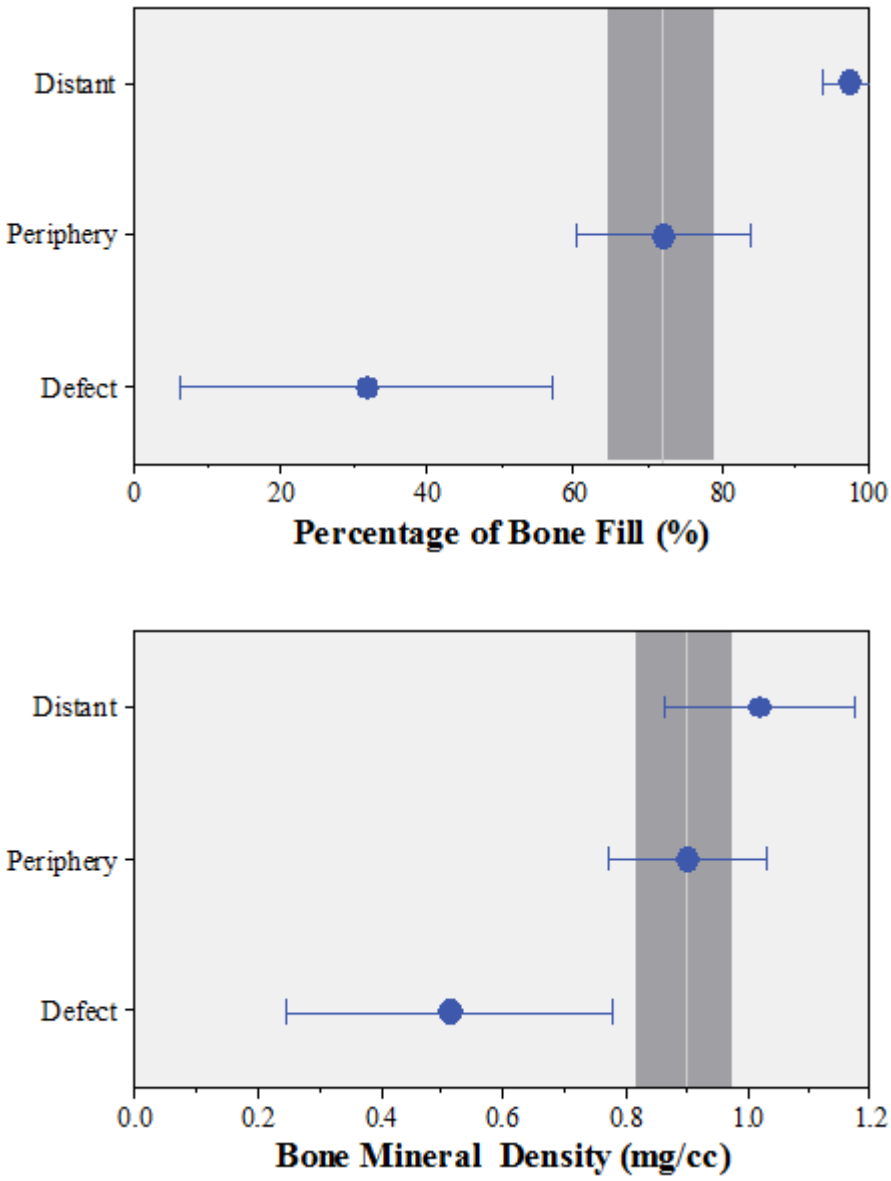

Figure 4. Equivalence Testing following 1st Generation Piezotome® Instrumentation. Equivalence testing using 95% confidence intervals for (a) percentage of bone fill (%) and (b) bone mineral density (mg/cc) as determined by μCT analysis for the three ROI following osteotomy fabrication with P1. For each treatment group, mean ± 95% confidence interval is charted. The dark gray zone represents the zone of indifference as determined by the mean ± one standard deviation following rotary instrumentation.

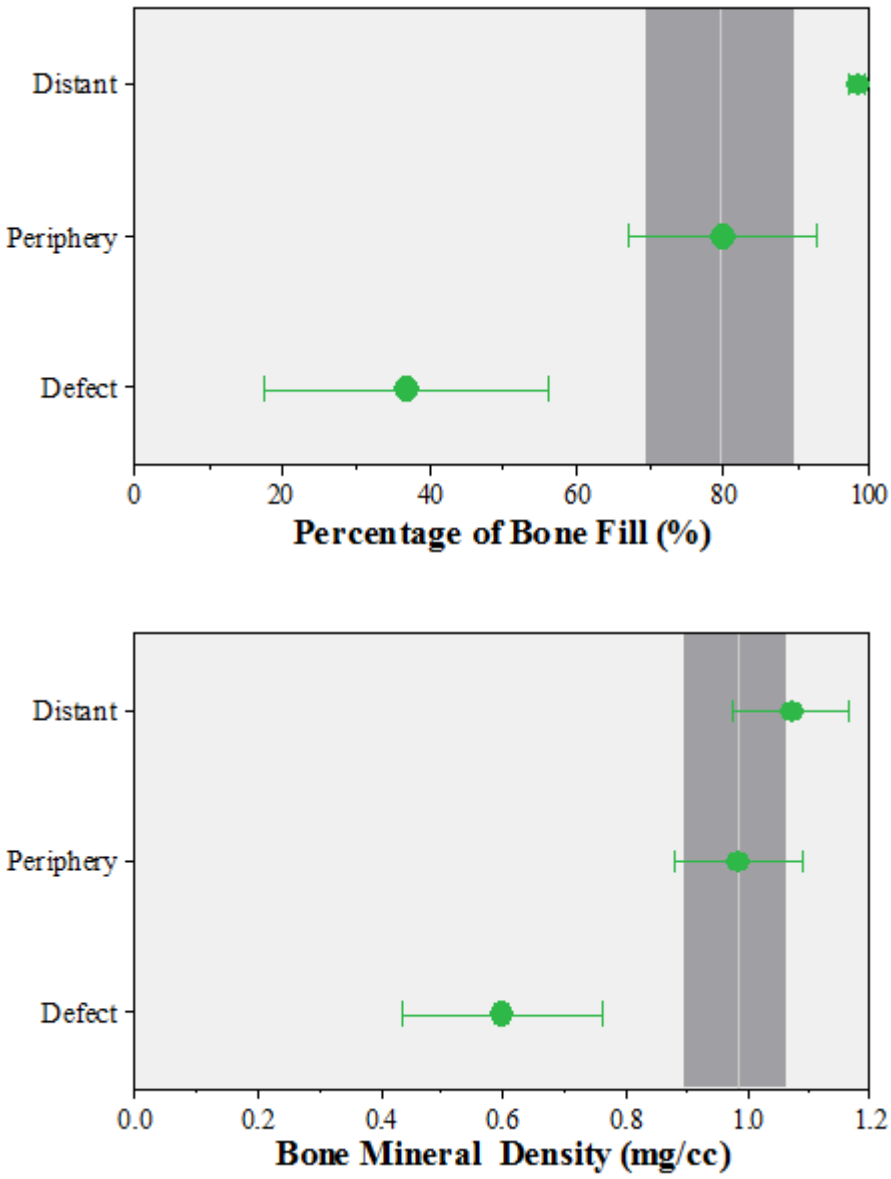

Figure 5. Equivalence Testing following 2nd Generation Piezotome® Instrumentation. Equivalence testing using 95% confidence intervals for (a) percentage of bone fill (%) and (b) bone mineral density (mg/cc) as determined by μCT analysis for the three ROI following osteotomy fabrication with P2. For each treatment group, mean ± 95% confidence interval is charted. The dark gray zone represents the zone of indifference as determined by the mean ± one standard deviation following rotary instrumentation.

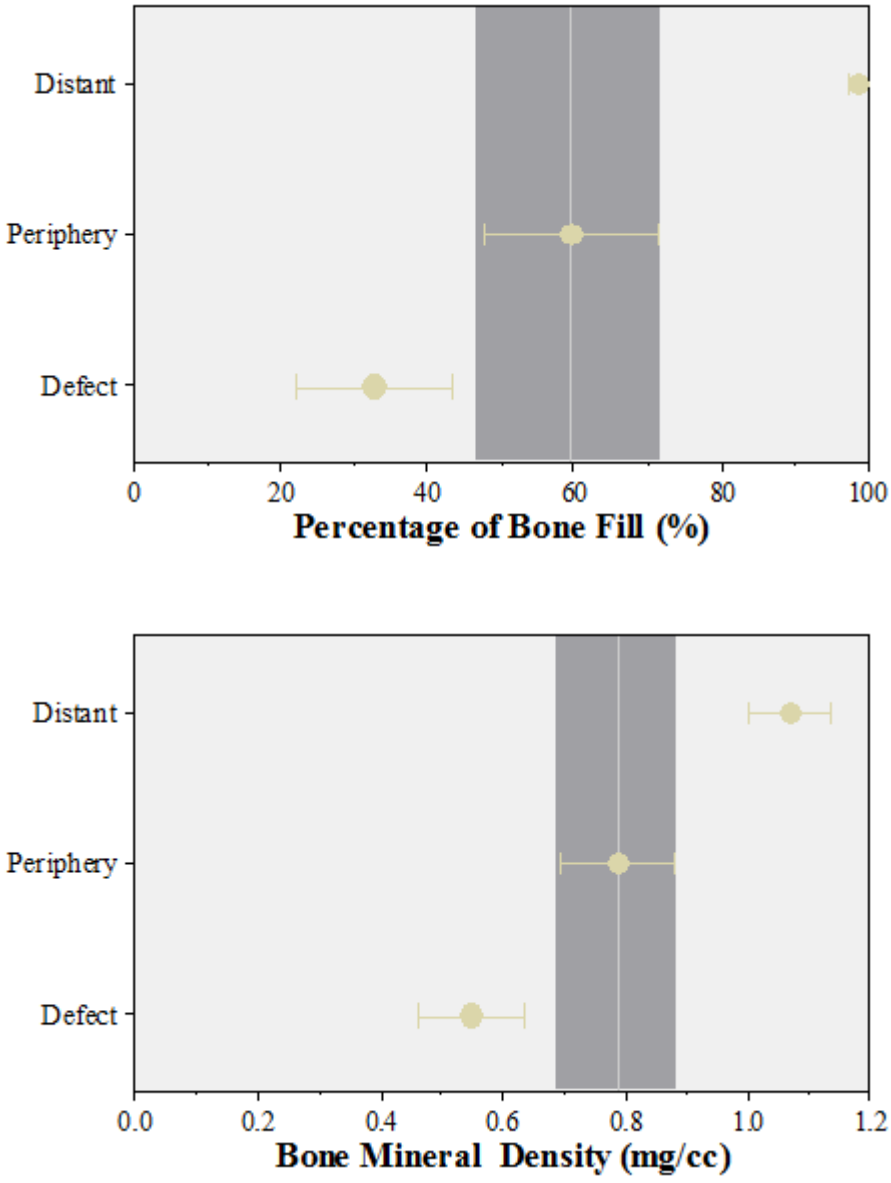

Figure 6. Equivalence Testing Following High Speed Rotary Instrumentation. Equivalence testing using 95% confidence intervals for (a) percentage of bone fill (%) and (b) bone mineral density (mg/cc) as determined by μCT analysis for the three ROI following osteotomy fabrication with R. For each treatment group, mean ± 95% confidence interval is charted. The dark gray zone represents the zone of indifference as determined by the mean ± one standard deviation following rotary instrumentation.